Article

Cell Reports

# Helminth Infections Suppress the Efficacy of Vaccination against Seasonal Influenza

## Graphical Abstract

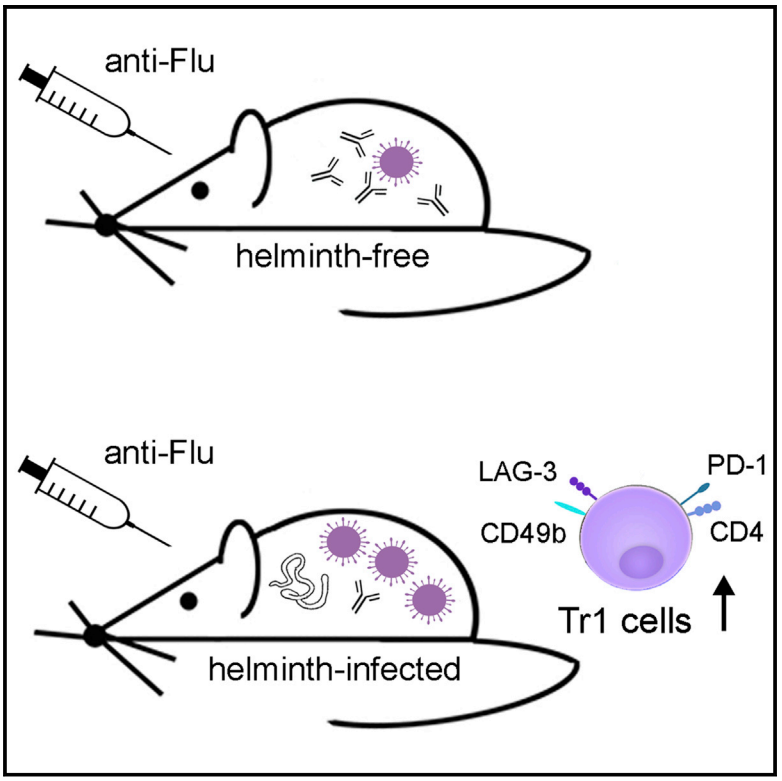


## Authors

Wiebke Hartmann, Marie-Luise Brunn, Nadine Stetter, ..., Stephanie Stanelle-Bertram, Gülsah Gabriel, Minka Breloer

## Correspondence

breloer@bnitm.de

## In Brief

Parasitic worms down-modulate the immune system of their host to establish chronic infections. Hartmann et al. demonstrate that this suppresses responsiveness to vaccinations against influenza. Mice with on-going or previously resolved helminth infections displayed a systemic increase of Tr1 cells and impaired vaccination efficacy that was partially mediated by IL-10.

## Highlights

- Underlying helminth infections impair efficacy of anti-influenza vaccination
- Vaccination responses are still impaired after termination of helminth infection
- Helminth infections induce sustained expansion of IL-10$^{+}$CD49b$^{+}$LAG3$^{+}$ Tr1 cells
- IL-10 blockade partially restores anti-influenza vaccination efficacy

Hartmann et al., 2019, Cell Reports *29*, 2243–2256
November 19, 2019 
https://doi.org/10.1016/j.celrep.2019.10.051

CellPress

Cell Reports
Article



# Helminth Infections Suppress the Efficacy of Vaccination against Seasonal Influenza

Wiebke Hartmann,[1] Marie-Luise Brunn,[1] Nadine Stetter,[1] Nicola Gagliani,[2,3] Franziska Muscate,[2] Stephanie Stanelle-Bertram,[4] Gülsah Gabriel,[4,5] and Minka Breloer[1,6,*]

[1]Section for Molecular Biology and Immunology, Bernhard Nocht Institute for Tropical Medicine, 20359 Hamburg, Germany
[2]I Department of Medicine and Department of General, Visceral and Thoracic Surgery, University Medical Center Hamburg-Eppendorf, 20246 Hamburg, Germany
[3]Immunology and Allergy Unit, Department of Medicine, Solna, Karolinska Institute and University Hospital, 17176 Stockholm, Sweden
[4]Research Department for Viral Zoonoses-One Health, Heinrich Pette Institute, Leibniz Institute for Experimental Virology, 20251 Hamburg, Germany
[5]Institute for Virology, University for Veterinary Medicine, Hannover, Germany
[6]Lead Contact
*Correspondence: breloer@bnitm.de
https://doi.org/10.1016/j.celrep.2019.10.051

## SUMMARY

**Helminth parasites infect more than a quarter of the human population and inflict significant changes to the immunological status of their hosts. Here, we analyze the impact of helminth infections on the efficacy of vaccinations using *Litomosoides sigmodontis*-infected mice. Concurrent helminth infection reduces the quantity and quality of antibody responses to vaccination against seasonal influenza. Vaccination-induced protection against challenge infections with the human pathogenic 2009 pandemic H1N1 influenza A virus is drastically impaired in helminth-infected mice. Impaired responses are also observed if vaccinations are performed after clearance of a previous helminth infection, suggesting that individuals in helminth-endemic areas may not always benefit from vaccinations, even in the absence of an acute and diagnosable helminth infection. Mechanistically, the suppression is associated with a systemic and sustained expansion of interleukin (IL)-10-producing $CD4^+CD49^+LAG\text{-}3^+$ type 1 regulatory T cells and partially abrogated by *in vivo* blockade of the IL-10 receptor.**

## INTRODUCTION

Helminths are large multicellular parasites that infect 2 billion people worldwide (Hotez et al., 2008). Despite the fact that helminth parasites can neither hide from their host's immune attack nor multiply within their definitive hosts, many helminths survive for decades causing chronic infections. To avoid their elimination and to limit immune pathology and thus restrict damaging their hosts, helminths have evolved sophisticated mechanisms to suppress their host's immune response (McSorley and Maizels, 2012). To this end, helminths exploit the intrinsic regulatory pathways that usually maintain homeostasis of the mammalian immune system (Maizels and McSorley, 2016). Because this immune suppression is not restricted to helminth-specific immune responses, a concurrent helminth infection may also interfere with the immune response to unrelated antigens such as vaccines. Accordingly, many human studies show a negative correlation between a diagnosed helminth infection and the cellular or humoral response to vaccinations (for review, see Borkow and Bentwich, 2008; Elias et al., 2006; Urban et al., 2007). On the other hand, several published studies reported diverse results or failed to record a significant correlation between helminth infection status and vaccination response. For instance, no correlation between pre-existing *Schistosoma mansoni* or any intestinal helminth infection and the antibody (Ab) response to a vaccination against human papillomavirus was observed (Brown et al., 2014). The Ab response to a malaria vaccine candidate was reduced in children with concurrent *Trichuris trichuria* infection, whereas *Ascaris lumbricoides* infection did not modulate the vaccination response (Esen et al., 2012). Drug-induced deworming, that elevated the Ab response to cholera vaccination in one study (Cooper et al., 2000), did not elevate responses to cholera, meningococcal, or influenza vaccination in other studies (Brückner et al., 2015, 2016).

To investigate these issues in a controlled setting, we use infection of mice with *Litomosoides sigmodontis* as a model for human helminth infections (Allen et al., 2008; Hoffmann et al., 2000). *L. sigmodontis* is a filarial parasite that is transmitted as infective third stage larvae (L3) during the blood meal of mites, the intermediate host, to the definitive host, the cotton rat. Laboratory mice can be naturally infected by exposure to L3 transmitting mites. L3 migrate within 4 days via the lymphatic system to the thoracic cavity (TC) and molt via a L4 to adult worms. Semi-susceptible C57BL/6 mice start to kill the parasites by granuloma formation after 45 days, whereas fully susceptible BALB/c mice stay infected for more than 90 days (Graham et al., 2005).

Using the thymus-dependent (TD) antigen Dinitrophenol coupled to keyhole limpet hemocyanin (DNP-KLH) as a model "vaccine," we have shown before that *L. sigmodontis* infection suppressed the IgG response to DNP-KLH "vaccination" in both BALB/c and C57BL/6 mice (Haben et al., 2014; Hartmann et al., 2011). We hypothesized that this helminth

infection-mediated suppression of Ab responses to model antigens would also apply for the protective Ab responses to vaccinations against actual pathogens such as influenza virus. Seasonal Influenza is predominantly elicited by circulating influenza virus A, and according to the World Health Organization (2019), causes up to half a million casualties each year. Disease can be prevented by a vaccination that elicits a neutralizing IgG response to the variable epitopes of the influenza hemagglutinin (HA) head (Dormitzer et al., 2011).

Here, we compare the efficacy of vaccinations against seasonal influenza that were licensed for humans during the seasons 2014/15 to 2016/17 in helminth-infected and non-infected mice. We show that helminth infections reduced the quantity and neutralizing quality of Ab responses to the vaccination and impaired the protection against a challenge infection with the human pathogenic 2009 pandemic H1N1 influenza A virus (2009 pH1N1) (Garten et al., 2009). Suppression of vaccination efficacy in helminth-infected mice was accompanied by a sustained and systemic expansion of type 1 regulatory T cells (Tr1) and dependent on interleukin (IL)-10. Importantly, even mice with a history of helminth infections displayed systemic Tr1 expansion and impaired responses to vaccinations performed after clearance of their acute helminth infection. Thus, our combined results strongly suggest that the population living in helminth endemic areas may not benefit from vaccinations even if individuals with previously treated and cleared helminth infections appear negative in helminth diagnosis at the moment of vaccination.

## RESULTS

### Acute Helminth Infection Suppresses Antibody Response to Vaccination against Influenza and Impairs Protection against Homologous Virus Challenge

Analyzing helminth-induced immune modulation, we have shown before that a concurrent infection with the helminth parasite *L. sigmodontis* suppressed the Ab response to immunization against the TD model antigen DNP-KLH in BALB/c and C57BL/6 mice (Haben et al., 2014; Hartmann et al., 2011). To test the clinical relevance of these findings, we compared the efficacy of vaccination against influenza in naive and helminth-infected mice (Figure 1). We used Begripal, a non-adjuvanted trivalent split subunit vaccine that is composed of HA derived from three different influenza strains including 2009 pH1N1 as vaccine against seasonal influenza. Vaccination of C57BL/6 mice elicited a HA-specific IgG response that was more than 5-fold suppressed by concurrent *L. sigmodontis* infection. Helminth infection reduced the quantity of both isotypes in response to vaccination, the Th1-associated HA-specific IgG2b/c and Th2-associated HA-specific IgG1 (Figure 1B). Accordingly, virus neutralizing capacity of the elicited Ab response, measured by hemagglutination inhibition assay (HI), was 10-fold reduced in the sera derived from helminth-infected, vaccinated mice compared to non-infected, vaccinated mice (Figure 1C). The human pathogenic Influenza A H1N1 A/HH/NY/1580/09 strain that replicates in mice without further adaptation (Maines et al., 2009; Otte and Gabriel, 2011; Otte et al., 2011) was used to perform homologous challenge infections. Intranasal infection with a sub-lethal virus dose induced transient weight loss in non-vaccinated mice, while vaccinated mice were completely protected (Figure 1D). Mice that were helminth-infected at the moment of vaccination displayed a statistically significant increased weight loss compared to the protected control group. Analysis of the influenza A viral burden revealed similar results (Figure 1E). Non-vaccinated mice displayed high viral burden in the lungs 3 days after an influenza challenge infection, regardless of the helminth infection status. Vaccination conferred sterile protection in 11 out of 15 control mice (73%) whereas only 4 out of 13 helminth-infected and vaccinated mice (31%) displayed sterile protection. Interestingly, within the non-vaccinated groups, helminth-infected mice displayed slightly reduced weight loss compared to non-infected mice although viral burden in the lungs were alike (Figures 1D and 1E, open circles to open squares). Finally we confirmed that the vaccination against influenza as such did not affect helminth parasite burden, as expected (Figure S1).

Immune competent, semi-susceptible C57BL/6 mice eradicate *L. sigmodontis* parasites between days 45 and 60 post infection (p.i.) (Graham et al., 2005). In our experimental setting, the influenza challenge infection is timed at day 45 of *L. sigmodontis* infection (Figure 1A) and thus may coincide with active helminth infection. Although this setting may well reflect the situation in the human population in helminth-endemic areas, we aimed to specifically analyze the protective capacity of the vaccination against influenza in control and helminth-infected mice without overlapping effects induced by an ongoing helminth/influenza co-infection. In a first approach, we transferred the sera of vaccinated control mice and vaccinated helminth-infected mice into "helminth-free" recipient mice that were infected with influenza subsequently (Figure S2A). We confirmed that HA-specific IgG titers were lower (5- to 10-fold) in sera derived from vaccinated *L. sigmodontis*-infected compared to sera derived from the vaccinated control group as expected (Figure S2B). Although this passive immunization did not protect as efficiently as the active vaccination against influenza that we performed as internal control, the mice that received serum derived from vaccinated control mice lost significantly less weight than mice that received either no serum or serum derived from helminth-infected, vaccinated mice (Figure S2C).

In a second approach, we allowed the helminth-infected, vaccinated mice to naturally clear the *L. sigmodontis*-infection before performing the influenza A virus challenge infection (Figure 2). To this end, non-infected and day 28 helminth-infected mice were vaccinated with Begripal. The reduced Ab response to vaccination in the helminth-infected group was confirmed at day 14 post vaccination regarding quantity of HA-specific IgG1, IgG2b, IgG2c (Figure 2B), and HI titer (Figure 2c), thus reproducing the results shown in Figure 1. Instead of an immediate influenza challenge infection, the mice were kept for additional 100 days. This allows eradication of *L. sigmodontis* in the formerly helminth-infected mice and simulates the elapsed time between seasonal influenza vaccination and "challenge" exposure in the human population. Analysis of sera from day 114 post vaccination against influenza showed that HA-specific Ab were still present at these late time points. Thereby, the quantity of HA-specific IgG1 and IgG2b/c (Figure 2D) and the neutralizing quality indicated by HI titer (Figure 2E) were reduced 2- to 5-fold in helminth-infected mice compared to non-infected

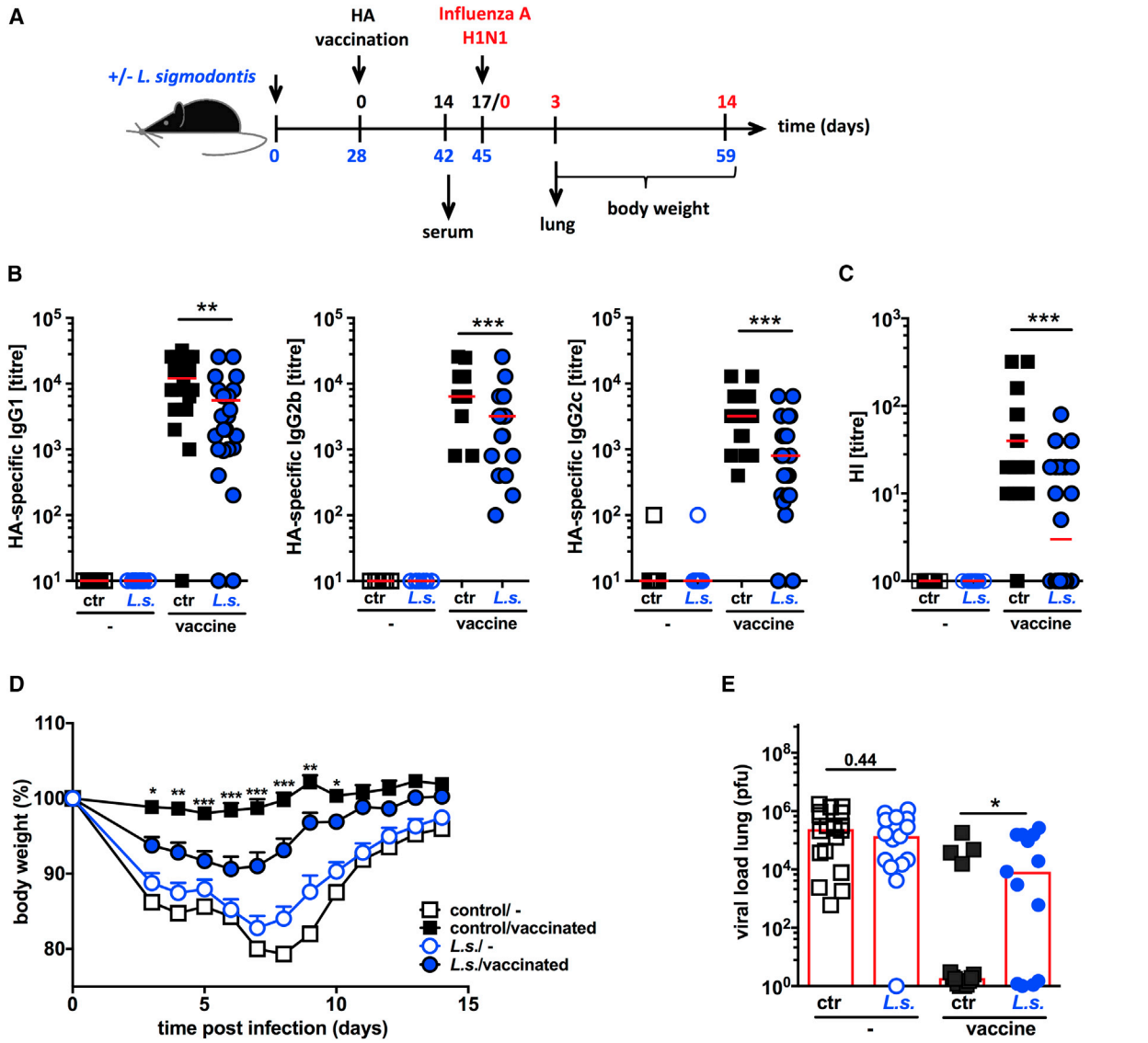


**Figure 1. Acute Helminth Infection Suppresses Antibody Response to Vaccination against Influenza and Protection against Homologous Virus Challenge**

(A) Experimental design: C57BL/6 mice were left naive (black squares) or infected with *L. sigmodontis* (blue circles). Mice either received a control injection (open symbols) or were i.p. vaccinated with Begripal at day 28 post *L. sigmodontis* infection (closed symbols).

(B) Titers of HA-specific IgG1, IgG2b, and IgG2c were quantified by ELISA 14 days after vaccination.

(C) HI was measured day 14 after vaccination. All mice were intranasally (i.n.) infected with Influenza A virus day 17 post vaccination.

(D and E) (D) Body weight was measured at the indicated time points, and (E) influenza virus burden in the lung was quantified.

(B–E) Combined results from 3 independent experiments with $n \geq 4$ per group, time point, and experiment. The lines in (B) and (C) show the median, and asterisks indicate statistically significant differences of the vaccinated control to the vaccinated *L. sigmodontis*-infected group (Mann-Whitney U test). Symbols in (D) represent the mean percentage of initial bodyweight for all mice, error bars show SEM, and asterisks indicate statistically significant differences of the mean of the control vaccinated group to the *L. sigmodontis*-infected vaccinated group (2-way ANOVA). The bars in (E) show the median, and asterisks indicate statistically significant differences of the control groups to *L. sigmodontis*-infected groups (Mann-Whitney U test). Each symbol represents an individual mouse. *$p \leq 0.05$, **$p \leq 0.01$, ***$p \leq 0.001$.

mice. Vaccinated mice were protected from weight loss induced by a subsequent influenza A virus challenge infection (Figure 2F), whereas mice that had been helminth-infected at the moment of vaccination lost statistically significant more weight than the vaccinated control group.

We used C57BL/6 mice for this study because they are more susceptible to 2009 pH1N1 influenza A virus infection than BALB/c mice that do not display a drastic weight loss upon influenza challenge infection (Otte and Gabriel, 2011). Nevertheless, we performed a proof of principle experiment to extend our

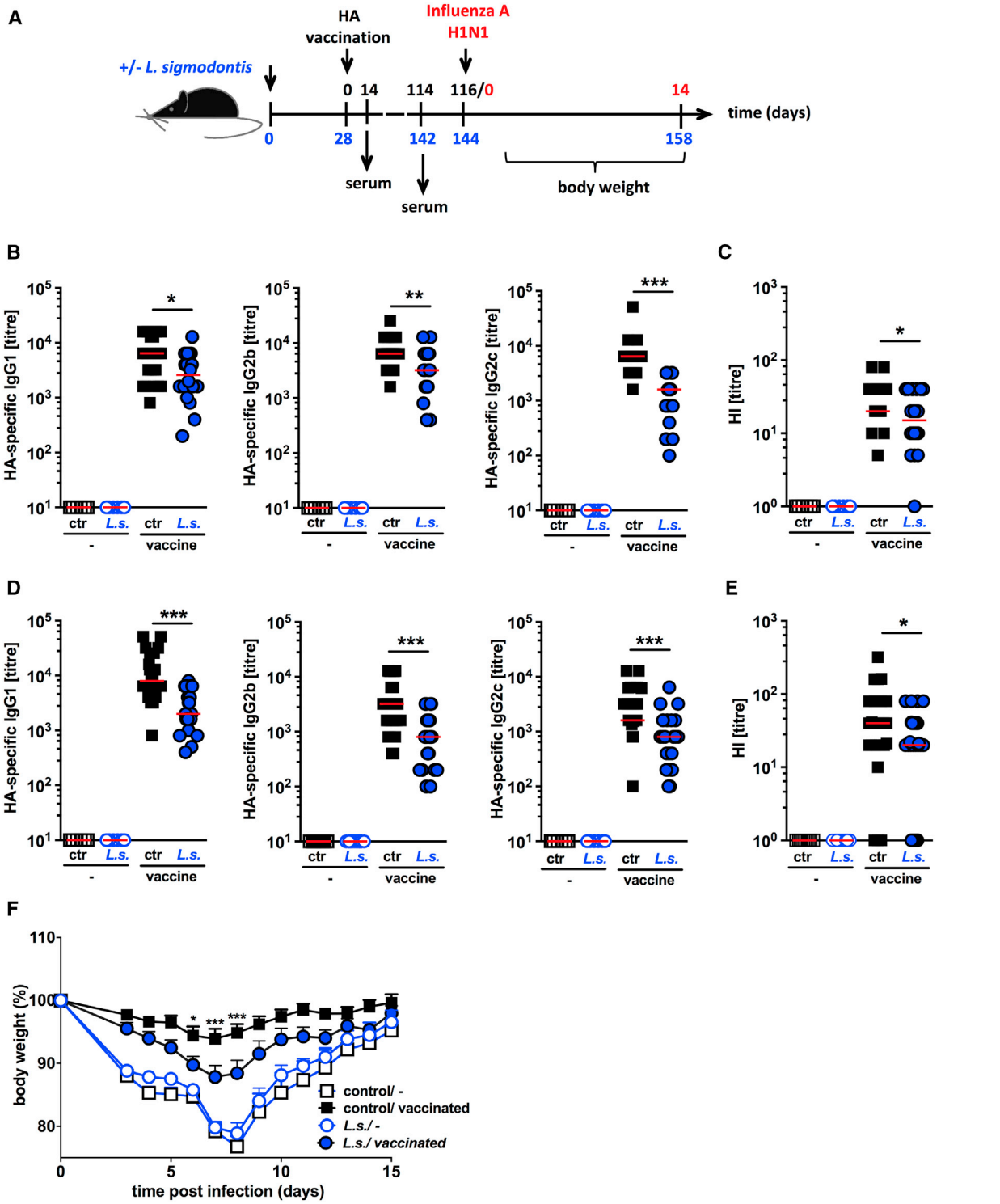


**Figure 2. Reduced Efficacy of Vaccination against Influenza in *L. sigmodontis*-Infected Mice on Late Challenge**

(A) Experimental design: C57BL/6 mice were left naive (black squares) or infected with *L. sigmodontis* (blue circles). Mice either received a control injection (open symbols) or were i.p. vaccinated with Begripal at day 28 post *L. sigmodontis* infection (closed symbols).

(B–E) HA-specific IgG1, IgG2b, and IgG2c and (C and E) HI titers were quantified 14 days (B and C), and 114 days (D and E) after vaccination. All mice were i.n. infected with Influenza A virus 2 days later. Combined results from 4 independent experiments with n ≥ 5 per group and experiment. The lines show the median and asterisks indicate statistically significant differences of vaccinated control to the vaccinated L. sigmodontis-infected groups (Mann-Whitney U test).

*(legend continued on next page)*

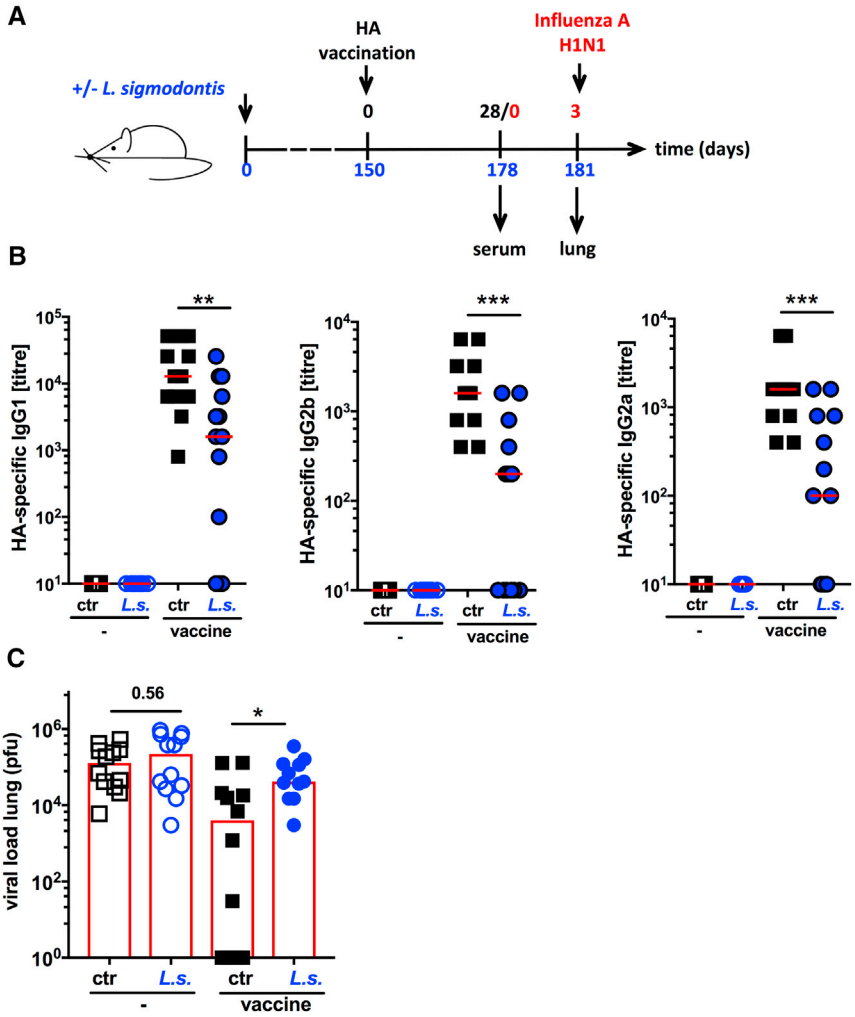


**Figure 3. Reduced Efficacy of Vaccination against Influenza in *L. sigmodontis*-Infected BALB/c Mice**

(A) Experimental design: BALB/c mice were left naive (black squares) or infected with *L. sigmodontis* (blue circles). Mice either received a control injection (open symbols) or were i.p. vaccinated Begripal at day 150 post *L. sigmodontis* infection (closed symbols).

(B) Titers of HA-specific IgG1, IgG2b, and IgG2a were quantified by ELISA 4 weeks after vaccination.

(C) All mice were i.n. infected with Influenza A virus and viral burden in the lung was quantified. Graphs show combined results from 2 experiments with n = 6 per group and experiment. Each symbol represents an individual mouse, the lines show the median and asterisks indicate statistically significant differences of the control groups to the *L. sigmodontis*-infected groups (Mann-Whitney U test). *p ≤ 0.05, **p ≤ 0.01, ***p ≤ 0.001.

observation to the fully susceptible BALB/c mouse model of *L. sigmodontis* infection (Figure 3). BALB/c mice, vaccinated at day 150 p.i., displayed the same reduction of HA-specific IgG1, IgG2b, and IgG2a response that was observed in C57BL/6 mice (Figure 3B). Challenge infection of BALB/c mice with a 10-fold higher 2009 pH1N1 influenza A virus dose compared to the one used for C57BL/6 mice resulted in replicating influenza virus in the lungs of non-vaccinated BALB/c mice (Figure 3C). Vaccination of the non-helminth-infected control group reduced viral burden, while vaccinated helminth-infected and non-vaccinated BALB/c mice displayed comparably high viral burden.

In conclusion, these results show that concurrent infection with the helminth parasite *L. sigmodontis* results in reduced quantity and quality of Ab response to a vaccination against seasonal influenza and impaired protection against a subsequent challenge infection with the human-pathogenic 2009 pH1N1 influenza A virus in C57BL/6 and BALB/c mice. The impaired protection against influenza challenge infection was predominantly mediated by the reduced neutralizing Ab response to vaccination and not dependent on the presence of viable helminths during influenza challenge infection.

## Sustained Suppression of Vaccination Response in Previously Helminth-Infected Mice

To analyze the kinetics of this helminth-induced suppression, we performed a pilot study comparing the response to vaccination at different time points post *L. sigmodontis* infection (Figure 4). Vaccination against influenza of day-30 infected C57BL/6 mice, containing viable helminths in the TC, resulted in suppressed HI response, re-iterating the results shown in Figures 1C and 2C. The same suppression of HI response to the vaccination against influenza was observed at day 60 post *L. sigmodontis*-infection (i.e., in mice that contained mostly killed and coated parasites) and at day 90 and 100 post initial *L. sigmodontis*-infection (i.e., in mice that had terminated their infection by granuloma formation and did not contain viable parasites at the moment of vaccination). The sustained suppression of vaccination response at day 100 post *L. sigmodontis*-infection was subsequently confirmed in two independent experimental repeats (Figure 4B, day 100).

(F) Body weight was measured at the indicated time points. Combined results from 2 independent experiments with n ≥ 6 per group, time point and experiment. Symbols represent the mean percentage of initial bodyweight for all mice in the indicated groups at indicated time points, error bar shows SEM, and asterisks indicate statistically significant differences of the control vaccinated group to the *L. sigmodontis*-infected vaccinated group (2-way ANOVA). Each symbol represents an individual mouse. *p ≤ 0.05, **p ≤ 0.01, ***p ≤ 0.001.

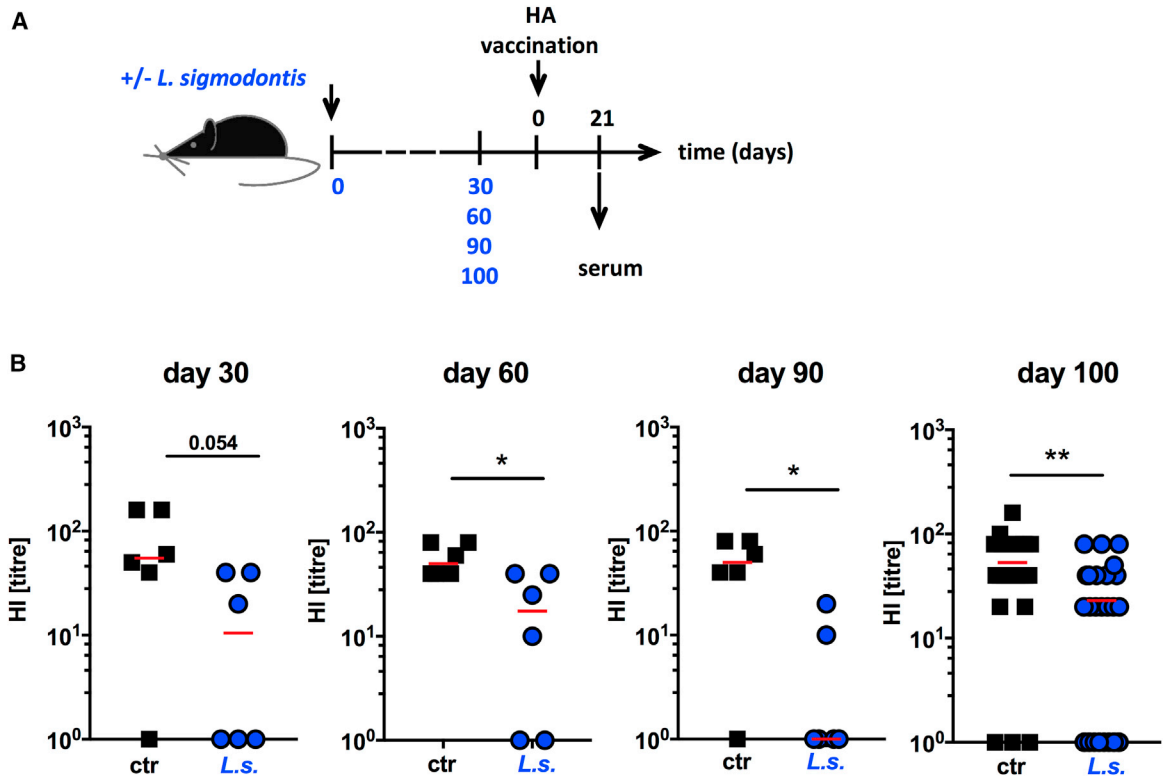


**Figure 4. Sustained Suppression of Vaccination Response in Previously *L. sigmodontis*-Infected Mice**

(A) Experimental design: C57BL/6 mice were left naive (black squares) or infected with *L. sigmodontis* (blue circles).

(B) Mice were i.p. vaccinated with Begripal at the indicated time points, and HI titers were quantified 3 weeks after vaccination. Graphs show combined results from 3 independent experiments (day 100) or one experiment (days 30, 60, 90) with n = 6 per group and experiment. Each symbol represents an individual mouse, the lines show the median, the numbers represent the p value, and asterisks indicate statistically significant differences of the vaccinated control group to the vaccinated *L. sigmodontis*-infected group (Mann-Whitney U test). *$p \leq 0.05$, **$p \leq 0.01$.

We have shown before that concurrent helminth infection impaired the proliferation of adoptively transferred T cells (Hartmann et al., 2015). Extending the kinetic analysis of helminth-induced suppression to T cell responses, we transferred T cell receptor transgenic OT-II T cells into day 14 and day 90 *L. sigmodontis*-infected C57BL/6 mice and recorded their antigen-specific proliferation *in vivo* (Figure S3). OT-II T cell proliferation was reduced in mice carrying viable helminths (day 14 p.i.) and in mice that had terminated their infection containing only remnants of killed helminths (day 90 p.i.) to the same extent (Figure S3C).

Taken together, these results show that helminth infection-induced suppression of B and T cell responses to unrelated bystander antigens was maintained in the absence of viable parasites. However, we cannot exclude that the presence of residual helminth-derived material contributed to immunosuppression at late time points such as day 90 or day 100 after initial infection.

## Prolonged Suppression of Vaccination Efficacy in Helminth-Infected Mice Is Associated with Sustained and Systemic Expansion of Tr1 Cells

We next aimed to identify the cellular mechanism(s) responsible for the prolonged suppression of vaccination responses. As our previous research supported an involvement of $CD4^+$ T cells in mediating immunosuppression during *L. sigmodontis* infection (Haben et al., 2013; Hartmann et al., 2015), we focused on regulatory T cell subsets. To this end, we compared the thoracic $CD4^+$ T cell compartment in non-infected (Figure 5A) and day 30 *L. sigmodontis*-infected C57BL/6 mice (Figure 5B) with regard to described regulatory T cell co-receptors using t-distributed statistic neighbor embedding (t-SNE). This analysis visualizes complex data in a 2D plot, thus allowing the identification of cell clusters with a similar expression pattern. We observed a $Foxp3^-$ $CD4^+$ T cell population that strongly co-expressed lymphocyte activation gene-3 (LAG-3), programmed cell death-1 (PD-1), and CD49b selectively in helminth-infected mice. Thereby PD-1 and CD49b were expressed on a broader population, while all $LAG\text{-}3^+$ T cells co-expressed PD-1 and CD49b in *L. sigmodontis*-infected mice. Expression of cytotoxic T lymphocyte-associated protein 4 (CTLA-4) was present in $Foxp3^+$ Treg cells from naive mice and increased in $Foxp3^+$ Treg cells from helminth-infected mice. Interestingly, a second and distinct CTLA-4-expressing T cell population occurred within the $CD4^+$ $Foxp3^-$ $LAG3^+$ $CD49b^+$ T cells selectively in helminth-infected mice. Neither B and T lymphocyte attenuator (BTLA) nor T cell immunoreceptor with Ig and ITIM

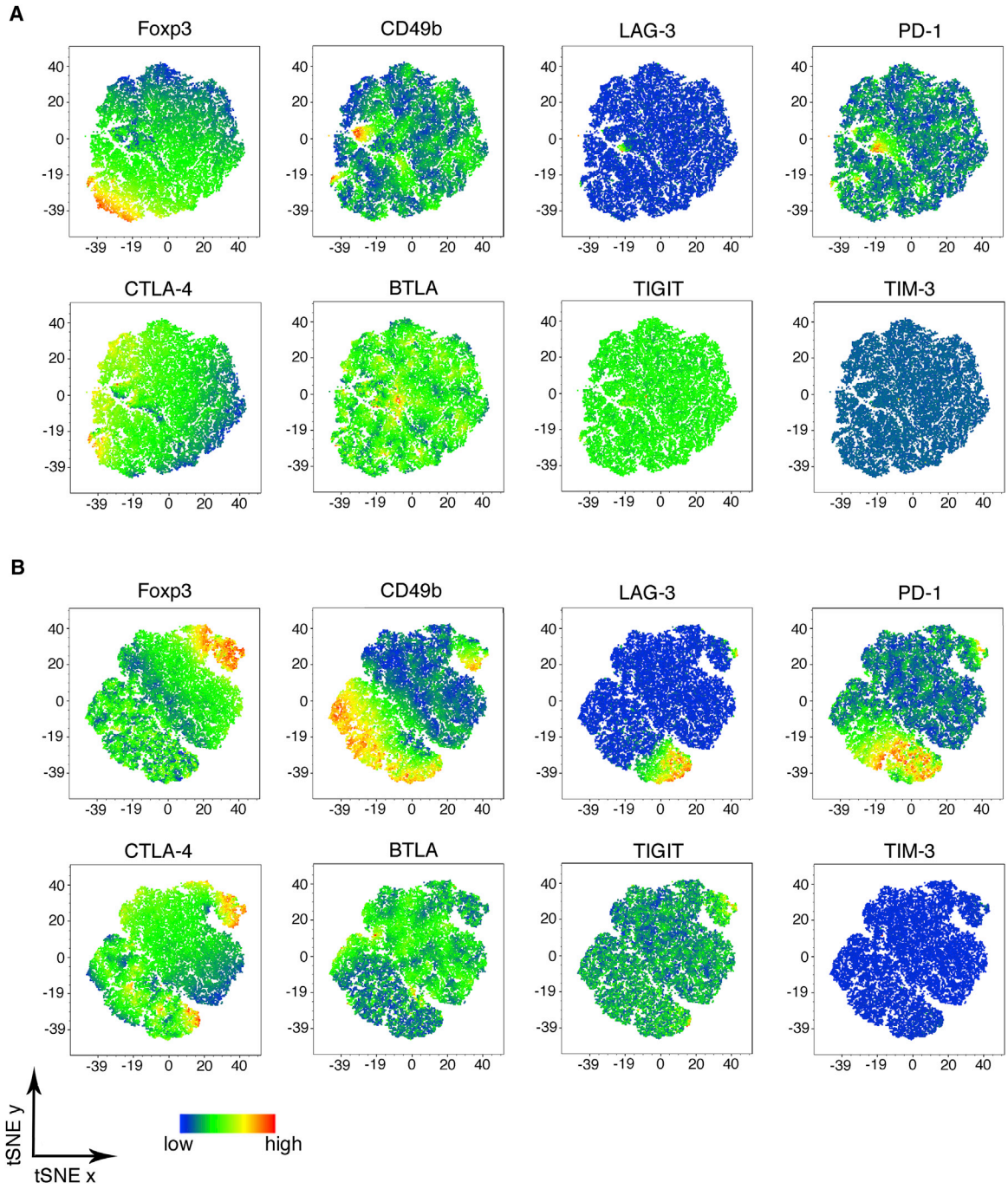


**Figure 5. *L. sigmodontis* Infection Increases the Expression of Regulatory Receptors in CD4$^+$ T Cells**

(A and B) C57BL/6 mice were left naive or infected with *L. sigmodontis.* TC cells were isolated and stained with a panel for regulatory receptors. Cells were analyzed on an LSRII. t-SNE calculation was performed with FlowJo. Representative t-SNE heatmaps generated from pre-gated CD4$^+$ T TC cells derived from naive (A) mice or mice infected for 30 days with *L. sigmodontis* (B) are shown for the expression of Foxp3, CD49b, LAG-3, PD-1, CTLA-4, BTLA, TIGIT, and TIM-3.

domains (TIGIT) or T cell immunoglobulin and mucin-domain containing-3 (TIM-3) were strongly regulated during *L. sigmodontis* infection.

Because co-expression of LAG-3 and CD49b on Foxp3$^-$ CD4$^+$ T cells characterizes type 1 regulatory T cells (Tr1) (Gagliani et al., 2013), we analyzed the dynamics of the Treg and Tr1 cell expansion during the course of *L. sigmodontis* infection in C57BL/6 mice (Figure 6). Tregs were identified as CD4$^+$ Foxp3$^+$ cells and Tr1 cells as CD4$^+$ Foxp3$^-$ LAG3$^+$ CD49b$^+$ cell population (Figure S4A). Treg numbers and

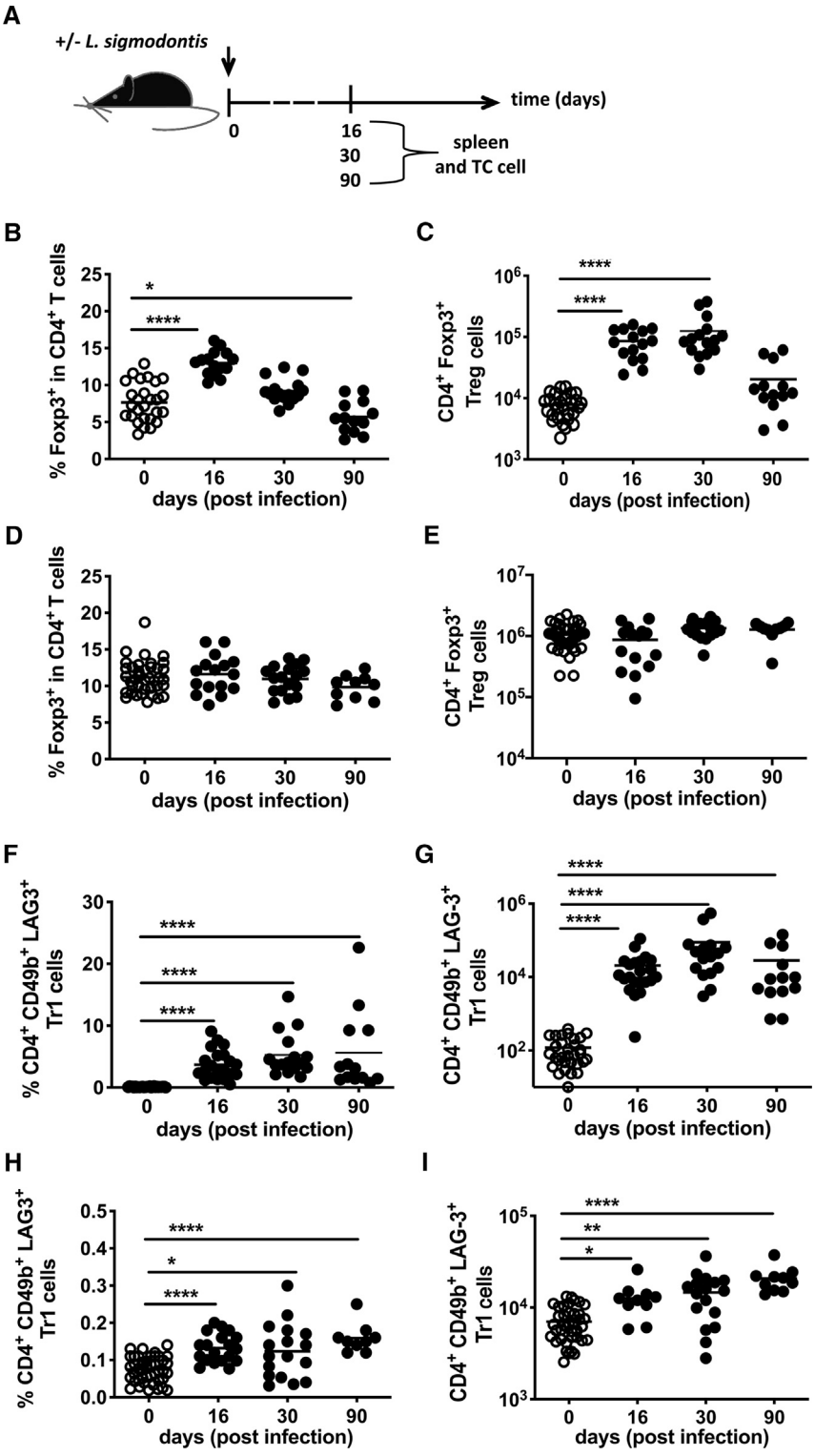


**Figure 6. *L. sigmodontis* Infection Induces Systemic and Sustained Expansion of Tr1 Cells**

(A) Experimental design: C57BL/6 mice were left naive (open circles) or infected with *L. sigmodontis* (closed circles). TC cells and splenocytes were stained at the indicated time points for expression of CD4, Foxp3, LAG-3, and CD49b and analyzed on a LSRII flow cytometer. The gating strategy is shown in the Figure S4A.

(B–I) Frequencies and total numbers of Treg (B–E) and Tr1 cells (F–I) in TC (B, C, F, and G) and spleen (D, E, H, and I). Shown are combined results from 2–4 experiments per time point with n $\geq$ 3 per experiment and group (n $\geq$ 2 for naive controls). Each symbol represents an individual mouse and the lines show the mean, and asterisks indicate statistically significant differences of the mean compared to non-infected mice (Kruskal-Wallis with Dunn's multiple comparison test). *p $\leq$ 0.05, **p $\leq$ 0.01, ***p $\leq$ 0.001, ****p $\leq$ 0.0001.

frequencies increased in the TC (Figures 6B and 6C) (i.e., at the site of helminth presence but not systemically in the spleen) (Figures 6D and 6E). Treg expansion in the TC was recorded at days 16 and 30 of *L. sigmodontis* infection (i.e., during the time points of acute infection). Treg numbers and frequencies returned to baseline at day 90 post *L. sigmodontis* infection (Figures 6B and 6C). By contrast, we recorded a sustained expansion of Tr1 cell numbers and frequencies, locally in the TC (Figures 6F and 6G) and systemically in the spleen (Figures 6H and 6I). Thereby, numbers and frequencies of Tr1 cells were still elevated at day 90 post initial *L. sigmodontis* infection, a time point when no viable worm was present and vaccination responses were still suppressed (Figure 4). This expansion of Tr1 cells in the spleens of *L. sigmodontis*-infected mice was not associated with changes in spleen cell numbers (Figure S5A). By contrast, cell numbers in the TC increased more than 10-fold throughout infection (Figure S5B).

Using IL-10/Foxp3 reporter mice, we verified that the CD4$^+$ Foxp3$^-$ LAG3$^+$ CD49b$^+$ Tr1 cells that expanded during *L. sigmodontis* infection at days 30 and 90 p.i. produce IL-10 (Figure S6). Thereby, frequencies and numbers of both IL-10-producing Foxp3$^-$ Tr1 cells and Foxp3$^+$ Tregs increased in the TC (Figures S6E and S6F) and spleen (Figures S6G and S6H) of day 30 *L. sigmodontis*-infected mice. We also quantified IL-10$^+$ regulatory B cells (Breg). We recorded a very low frequency of IL-10 expressing CD19$^+$ B cells that was unchanged in spleens and TC of non-infected and *L. sigmodontis*-infected mice (Figures S6E and S6G). Numbers of IL-10$^+$ CD19$^+$ B cells expanded in the TC of day 30 *L. sigmodontis*-infected mice,

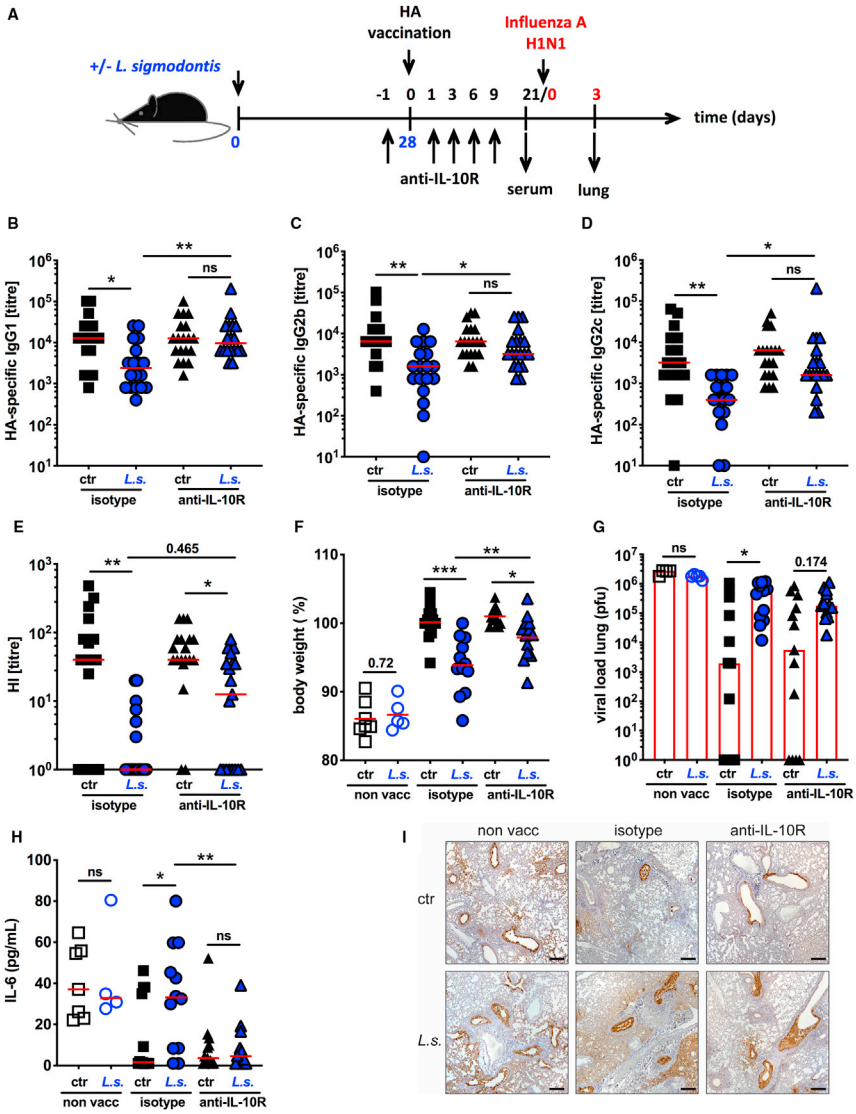


**Figure 7. Suppression of Vaccination Efficacy in Helminth-Infected Mice Is Mediated by IL-10**

(A) Experimental design: C57BL/6 mice were left naive (black squares, triangles) or infected with *L. sigmodontis* (blue circles, triangles). Mice were i.p. vaccinated with Begripal at day 28 post *L. sigmodontis* infection (closed symbols) or left naive (open symbols). All mice received additional i.p. injections of rat IgG isotype control (circles/squares) or anti-IL-10R mAb.

(B–E) Titers of (B) HA-specific IgG1, (C) IgG2b, (D) IgG2c, and (E) HI titer were quantified day 21 post vaccination. Sera from non-vaccinated groups mice did not contain detectable amount of HA-specific Ab and are not shown. All mice were i.n. infected with Influenza A virus and sacrificed 3 days later.

(F–H) (F) Body weight change at day 3 post influenza infection compared to starting weight was calculated and (G) influenza virus burden and (H) IL-6 content of lungs were quantified.

(I) Immunohistochemical analysis of lung sections 3 days after influenza challenge infection. A representative picture is shown for each group, scale bar is 200 μm.

Graphs show combined results from 3 (B–E), 2 (F–H), or 1 (I) independent experiment with n = 6 per group and experiment. Each symbol represents an individual mouse, the lines show the median (B–E, G, and H) or the mean (F), numbers indicate p value, and asterisks indicate statistically significant differences of the indicated groups. Kruskal-Wallis with Dunn's multiple comparison test (B–E, G, and H) or one-way ANOVA with Bonferroni's multiple comparison test (F). *p ≤ 0.05, **p ≤ 0.01, ****p ≤ 0.001.

but we did not record a systemic expansion of IL-10$^+$ CD19$^+$ B cell numbers in the spleen using either IL-10 reporter mice (Figures S6F and S6H) or intracellular IL-10 staining (Figure S6I).

## Suppression of Vaccination Efficacy in Helminth-Infected Mice Is Mediated by IL-10

To provide a causal link between the systemic and prolonged Tr1 expansion in helminth-infected mice and the impaired response to vaccination, we neutralized the dominant Tr1 cell cytokine IL-10 (Brockmann et al., 2017; Roncarolo et al., 2014) by *in vivo* blockade of the IL-10 receptor (IL-10R) (Figure 7). Injection of a neutralizing anti-IL-10R monoclonal antibody (mAb) during vaccination against influenza restored the HA-specific IgG1, IgG2b, and IgG2c response in helminth-infected mice to the level of the non-helminth-infected control group (Figures 7B–7D). The neutralization of IL-10-mediated signaling elevated also the HI titer of helminth-infected and vaccinated mice. However, the HI titers were still more than 2-fold reduced compared to non-infected vaccinated mice (Figure 7E). To analyze the efficacy of vaccination, we performed 2009 pH1N1 influenza A virus challenge infections with all groups including non-vaccinated control mice. Influenza infection-induced weight loss was ameliorated in vaccinated, helminth-infected mice under IL-10R blockade compared to vaccinated, helminth-infected mice with undisturbed IL-10R signaling (Figure 7F). However, vaccinated, helminth-infected mice still lost statistically significant more weight than vaccinated, non-helminth-infected control mice. By contrast, the neutralization of IL-10R abrogated the statistically significant differences in viral burden (Figure 7G) and IL-6 production (Figure 7H) in the lungs of helminth-infected mice compared to non-infected control mice. Immunohistochemical analysis of the lungs supported these findings (Figure 7I). Non-vaccinated groups infected with influenza A virus displayed similar viral antigen positive cells in bronchial and alveolar epithelium irrespective of prior helminth infection. In contrast, vaccinated and helminth-infected mice showed more viral antigen positive pulmonary cells compared to the group that was vaccinated in the absence of helminth infection. These differences in viral burden between vaccinated non-infected and helminth-infected groups were largely abolished upon IL-10R blockade.

To additionally control for a contribution of the IL-10-producing Tregs that expanded during *L. sigmodontis* infection (Figures S6F and S6H), we used the depletion of regulatory T cell (DEREG) mouse model (Lahl et al., 2007). Injection of DT into DEREG mice induces a transient depletion of Foxp3$^+$ Treg cells for 1–2 weeks, whereas DT-treated non-transgenic littermates retained normal Treg frequencies (Figure S7). Transient depletion of Tregs, either at the moment of *L. sigmodontis* infection or at the moment of vaccination, did not restore the response to vaccination against influenza. The vaccination-induced HI was more than 5-fold reduced in *L. sigmodontis*-infected mice compared to non-infected mice in the absence or presence of Foxp3$^+$ Tregs.

In summary, these findings show that helminth-induced suppression of vaccination efficacy was partly dependent on IL-10R-mediated signaling but independent of Tregs and thus supports the notion that the expanding IL-10 producing Tr1 cells contributed to this suppression.

## DISCUSSION

Human studies analyzing the impact of helminth infection on the immune response to vaccinations often lead to inconsistent results that most likely reflect the genetic heterogeneity of the study population, the difficulty in exact diagnosis of the helminth infection status, the presence of putatively undetected co-infections, and the undeterminable infection history of the study subjects. In the present study, we use mouse models allowing us to control each of these parameters to test if a concurrent helminth infection would compromise vaccination efficacy.

We report that a concurrent helminth infection caused a drastic reduction in the quantity and the neutralizing quality of the Ab response to vaccination against seasonal influenza. Notably, the Ab response to the vaccination was not polarized toward a Th2 phenotype but genuinely suppressed as both, Th1-associated IgG2 and the Th2-associated IgG1 response were reduced in helminth-infected mice. Furthermore, suppression was observed in BALB/c and C57BL/6 mice despite the different duration and outcome of the *L. sigmodontis* infection in both mouse strains. These findings agree with our previous studies analyzing the Ab response to TD model antigen immunizations in BALB/c and C57BL/6 mice (Haben et al., 2014; Hartmann et al., 2011). Likewise, chronic infections with the liver fluke *S. mansoni* or the intestinal helminth parasite *H. polygyrus* led to reduced IgG1 and IgG2 responses to either protein- or DNA-based anti-HIV (Dzhivhuho et al., 2018) and anti-malaria (Noland et al., 2010; Su et al., 2006) vaccination. A multiple co-infection with a combination of murine viruses (MHV68, MCMV, and mouse Influenza WSN) and *H. polygyrus* reduced the quantity of Ab response (Reese et al., 2016).

Using trivalent non-adjuvanted split subunit vaccines against influenza that were licensed for humans during the seasons 2014–2017, we demonstrate the clinical relevance of this bystander suppression during challenge infections with a patient isolate of the 2009 pH1N1 influenza A virus (Garten et al., 2009). Mice that were vaccinated while carrying an acute *L. sigmodontis* infection displayed increased weight loss and increased viral burden in the lung compared to mice vaccinated in the absence of helminth infection. We differentiate the impact of impaired Ab response to vaccination from the impact of the helminth/influenza co-infection by (1) performing passive immunizations and by (2) delaying the moment of influenza challenge infection of helminth-infected and vaccinated mice to a point in time after termination of the helminth infection. Thereby, we provide evidence that the helminth infection-induced reduction of the Ab response to the vaccination against influenza led to a more pronounced pathology during influenza A virus challenge infection. This holds true for both settings, the simultaneous presence of helminths and influenza virus, and the absence of an active helminth co-infection. We do not exclude, however, that a concurrent helminth infection would modulate the viral burden and/or pathology during an influenza challenge infection. Depending on the context, helminth co-infections were shown to increase the pathology of subsequent virus infections by suppressing the protective immune response (Dietze et al., 2016; Osborne et al., 2014; Reese et al., 2014), or to ameliorate pathology either by improving innate anti-viral immune responses (McFarlane et al., 2017) or by down-modulation of the virus infection-induced inflammation (Furze et al., 2006; Schuijs et al., 2016). Examining the body weight of non-vaccinated mice during the influenza virus challenge infection, we observed a slightly reduced weight loss in helminth-infected mice compared to non-helminth-infected mice although viral burden in the lung were unchanged (Figures 1D and 1E). This observation may reflect an amelioration of influenza infection-induced pathology in helminth co-infected mice. However, the net effect of the underlying helminth infection during vaccination clearly results in impaired protection, as we have shown here, employing a vaccination scheme that is commonly used for the human population.

Moreover, our kinetic analyses demonstrate that the suppressive status induced by helminths was preserved in the absence of viable parasites until after termination of the acute infection. C57BL/6 mice that were vaccinated 100 days after *L. sigmodontis* infection and had killed the helminth parasite by granuloma formation still displayed a reduced neutralizing Ab response to the vaccination against influenza. In addition, we have reported previously that Ab responses to model antigen immunization in BALB/c mice were still suppressed if immunization was performed 4 months after termination of *L. sigmodontis* infection (Haben et al., 2014).

These observations raise the mechanistic question of how the presence of a parasitic worm in the TC is translated to the reduction of B cell responses at a different site (to a vaccination applied i.p.) and at a later point in time (past the acute helminth infection). A recent study reported that intestinal *H. polygyrus* infection resulted in the atrophy of peripheral lymph nodes causing impaired cellular response to subsequent subcutaneous bacillus Calmette-Guérin (BCG) immunization (Feng et al., 2018). In our study, vaccination was performed i.p. and would target the spleen. Because the number of spleen cells remained unchanged during *L. sigmodontis* infection, we consider atrophy of lymphoid organs an unlikely explanation of the reduced influenza-specific B cell responses observed in *L. sigmodontis*-infected mice.

An unbiased t-SNE-based analysis highlighted Foxp3$^-$ CD49b$^+$ LAG-3$^+$ Tr1 cells as a distinct population that expanded

specifically in *L. sigmodontis*-infected mice. Tr1 cells expanded locally, but also systemically, in the spleen, a pre-requisite for inflicting systemic suppression to the vaccination applied i.p. Most importantly, kinetic analyses showed that these Foxp3$^-$ CD49b$^+$ LAG-3$^+$ Tr1 cells remained expanded in the absence of viable helminths 90 days after initial infection. Tr1 cells represent a rather heterogeneous cell population (Roncarolo et al., 2018), and IL-10 production by T cells per se is not indicative of a suppressive phenotype (Brockmann et al., 2018). However, the combination of the negative regulatory receptors LAG-3 and CD49b has been shown to identify the specific subpopulation of suppressive CD4$^+$ T cells (Brockmann et al., 2018; Gagliani et al., 2013). For these Tr1 cells, the cytokine IL-10 clearly contributed to anti-inflammatory effects in murine models of inflammatory bowel disease (Brockmann et al., 2017, 2018). Because no murine models for Tr1 cell depletion exist to date, we used neutralization of IL-10 as a rough indicator for a mechanistic contribution of the IL-10$^+$ Foxp3$^-$ CD49b$^+$ LAG-3$^+$ Tr1 cells to the suppressed vaccination response in *L. sigmodontis*-infected mice. Blockade of IL-10 signaling by application of neutralizing mAb to the IL-10 receptor partially abrogated the suppressive effect of the helminths. While the quantity of Ab response to vaccination was completely restored, the neutralizing Ab response was clearly elevated although still lower than in non-helminth-infected and vaccinated mice. The protection from influenza A virus challenge infection indicated by weight loss was also improved, and differences in lung viral burden and virus infection-induced IL-6 were no longer significant in helminth-infected, vaccinated mice under IL-10R blockade. This incomplete restoration of the vaccination efficacy can be explained by the plethora of molecular pathways Tr1 cells employ to exert anti-inflammatory effects in addition to IL-10 secretion such as negative regulation via co-inhibitory receptors (Roncarolo et al., 2014).

It should be pointed out that we performed the neutralization of IL-10R at day 28 of *L. sigmodontis* infection only. Thus, we have not formally shown that the suppression of vaccination response that we observed at later time points (i.e., day 100 of *L. sigmodontis* was also dependent on functional IL-10R signaling), although it was correlated to sustained and systemic expansion of IL-10-producing Tr1 cells. Moreover, we recognize that our approach to block IL-10 is not Tr1-specific because many cell types can produce IL-10, most importantly Foxp3$^+$ Treg, and Breg. IL-10$^+$ B cells contributed to bystander suppression in *S. mansoni*-infected mice (Mangan et al., 2004; Smits et al., 2007; for review, see Floudas et al., 2016; Hussaarts et al., 2011). We have shown before that *L. sigmodontis*-infection suppressed OT-II T cell proliferation *in vivo* only if the host's T cells were able to produce IL-10 (Hartmann et al., 2015). Likewise, T cell-derived IL-10, but not B cell-derived IL-10, mediated immune evasion during *L. sigmodontis* infection of C57BL/6 mice (Haben et al., 2013). Thus, the combined evidence of our previous studies suggests that T cell-derived IL-10 mediates suppression in *L. sigmodontis*-infected mice. Consenting with these findings, the frequencies of IL-10$^+$ B cells in either spleen or TC did not change during *L. sigmodontis* infection. However, because we observed a strong increase in the numbers of IL-10$^+$ B cells in the TC, we cannot formally rule out a contribution of Breg-derived IL-10 to suppression of vaccination responses against influenza because this was not addressed specifically in this study.

We also recorded a systemic expansion of IL-10$^+$ Foxp3$^+$ Tregs during *L. sigmodontis* infection that exceeded the IL-10$^+$ Tr1 cells in numbers. However, transient depletion of Foxp3$^+$ Tregs either at the time point of infection, or at the time point of vaccination, did not restore vaccination efficacy in this study. In line with these findings, we have shown previously that transient Foxp3$^+$ Treg depletion did neither restore the Ab response to model antigen immunization (Haben et al., 2014) nor the proliferation of adoptively transferred OT-II T cells (Hartmann et al., 2011). As the DEREG mouse model induces only transient Treg depletion for 1–2 weeks, we cannot formally exclude that repopulating Tregs would contribute to the suppression of the final Ab response.

In summary, our findings agree with a helminth-mediated induction of Foxp3$^-$ CD49b$^+$ LAG-3$^+$ Tr1 cells that partially expressed PD-1 and CTLA-4, produced IL-10, and subsequently contributed to impaired vaccine efficacy due to reduced neutralizing Ab responses. In line with this reasoning, IL-10$^+$ Tr1 cells were shown to suppress the IgG production by human B cells *in vitro* and in lymphopenic RAG$^{-/-}$ mice refilled with ovalbumin-specific T cells and B cells *in vivo* (Facciotti et al., 2016). Human Tr1 cells, derived from PBL of patients infected with the filarial parasite *Onchocerca volvulus* have been shown to skew the humoral response toward the regulatory isotype IgG4 (Satoguina et al., 2005, 2008).

From the translational point of view, our results strongly suggest that vaccines that are developed and tested for efficacy in the western world may by less efficient in helminth endemic areas. This is supported by a study that followed the response to vaccination with the seasonal influenza vaccine Begrivac (2004/2005) in Gabonese schoolchildren (van Riet et al., 2007). Children living in rural areas with high incidence of helminth infection displayed reduced H1N1-specific Ab responses to Begrivac compared to children living in semi-urban areas with lower incidence. Since the influenza pandemic in 2009 caused the highest mortality in Africa (Dawood et al., 2012), helminth-induced interference with vaccination efficacy and possible counter measures are of global relevance and clearly understudied so far. Therefore, the termination of helminth infection by drug-induced deworming has already been suggested as a strategy to improve vaccination responses. Murine studies revealed divergent results regarding the restoration of full responsiveness to vaccination after drug-induced deworming revealing refractory times in the range from 1 to 8 weeks (Da'dara and Harn, 2010; Su et al., 2006). Even the partial restoration of the cellular response to anti-HIV vaccination in *S. mansoni*-infected mice by praziquantel treatment did not abrogate the suppression of Ab response to the HIV gp140 protein (Dzhivhuho et al., 2018). Although some human studies reported the improvement of the humoral response to cholera vaccination upon deworming (Cooper et al., 2000), others did not, probably just reflecting inefficient anti-helminth treatment (Brückner et al., 2015, 2016). A comprehensive double-blind and placebo-controlled study reported a clear elevation of pro-inflammatory responses to *plasmodium*-infected erythrocytes 9 and 21 months after the onset

of a 3-monthly albendazole treatment scheme, while responses to vaccination were not addressed (Wammes et al., 2016). Agreeing with our findings, the deworming did not change the frequencies of Foxp3$^+$ Tregs in the PBL of the study subjects but reduced the frequency of Foxp3$^-$ CTLA-4$^+$ CD4$^+$ T cells that may well represent Tr1-like cells. Hence, the expansion of Tr1 cells rather than diagnosis of acute helminth infection may be indicative of a suppressed phenotype. Because the collective data of our study strongly suggest that (1) an underlying helminth infection would compromise vaccination responses, and (2) even after successful treatment, the formerly helminth-infected individuals may not respond efficiently to vaccination for some time, the diagnosis of a suppressed phenotype would be important for the estimation of vaccination success in helminth endemic areas.

## STAR★METHODS

Detailed methods are provided in the online version of this paper and include the following:

- KEY RESOURCES TABLE
- LEAD CONTACT AND MATERIALS AVAILIBILITY
- EXPERIMENTAL MODEL AND SUBJECT DETAILS
  - Mice
  - Cell Culture
- METHOD DETAILS
  - L. sigmodontis and influenza infection
  - Vaccination and quantification of the vaccine-specific humoral response
  - Quantification of HA-specific IgG
  - Hemagglutinin inhibition (HI) assay
  - Detection of viral loads and IL-6 in the lungs
  - Histology
  - Flow cytometry
  - Analysis of OT-II cell proliferation *in vivo*
- QUANTIFICATION AND STATISTICAL ANALYSIS
  - Statistical analysis
- DATA AND CODE AVAILABILITY

### SUPPLEMENTAL INFORMATION

Supplemental Information can be found online at https://doi.org/10.1016/j.celrep.2019.10.051.

### ACKNOWLEDGMENTS

We thank Gundula Pilnitz-Stolze for support with the immunohistochemical staining of murine lungs and Casey Weaver for sharing the 10BiT mice. This work was funded by the German research association DFG (BR 3754/2-2).

### AUTHOR CONTRIBUTIONS

Conceptualization, M.B., W.H., and G.G. (virology); Methodology, Investigation, Resources, and Data Analysis, W.H., M.-L.B., N.S., N.G., F.M., S.S.-B., G.G., and M.B.; Writing – Original Draft, M.B.; Writing – Editing, M.B., G.G., and W.H.; Funding Acquisition, M.B.

### DECLARATION OF INTERESTS

The authors declare no competing interests.

Received: March 11, 2019
Revised: August 29, 2019
Accepted: October 10, 2019
Published: November 19, 2019

### REFERENCES

Allen, J.E., Adjei, O., Bain, O., Hoerauf, A., Hoffmann, W.H., Makepeace, B.L., Schulz-Key, H., Tanya, V.N., Trees, A.J., Wanji, S., and Taylor, D.W. (2008). Of mice, cattle, and humans: the immunology and treatment of river blindness. PLoS Negl. Trop. Dis. *2*, e217.

Borkow, G., and Bentwich, Z. (2008). Chronic parasite infections cause immune changes that could affect successful vaccination. Trends Parasitol. *24*, 243–245.

Brockmann, L., Gagliani, N., Steglich, B., Giannou, A.D., Kempski, J., Pelczar, P., Geffken, M., Mfarrej, B., Huber, F., Herkel, J., et al. (2017). IL-10 Receptor Signaling Is Essential for TR1 Cell Function In Vivo. J. Immunol. *198*, 1130–1141.

Brockmann, L., Soukou, S., Steglich, B., Czarnewski, P., Zhao, L., Wende, S., Bedke, T., Ergen, C., Manthey, C., Agalioti, T., et al. (2018). Molecular and functional heterogeneity of IL-10-producing CD4$^+$ T cells. Nat. Commun. *9*, 5457.

Brown, J., Baisley, K., Kavishe, B., Changalucha, J., Andreasen, A., Mayaud, P., Gumodoka, B., Kapiga, S., Hayes, R., and Watson-Jones, D. (2014). Impact of malaria and helminth infections on immunogenicity of the human papillomavirus-16/18 AS04-adjuvanted vaccine in Tanzania. Vaccine *32*, 611–617.

Brückner, S., Agnandji, S.T., Berberich, S., Bache, E., Fernandes, J.F., Schweiger, B., Massinga Loembe, M., Engleitner, T., Lell, B., Mordmüller, B., et al. (2015). Effect of Antihelminthic Treatment on Vaccine Immunogenicity to a Seasonal Influenza Vaccine in Primary School Children in Gabon: A Randomized Placebo-Controlled Trial. PLoS Negl. Trop. Dis. *9*, e0003768.

Brückner, S., Agnandji, S.T., Elias, J., Berberich, S., Bache, E., Fernandes, J., Loembe, M.M., Hass, J., Lell, B., Mordmüller, B., et al. (2016). A single-dose antihelminthic treatment does not influence immunogenicity of a meningococcal and a cholera vaccine in Gabonese school children. Vaccine *34*, 5384–5390.

Cooper, P.J., Chico, M.E., Losonsky, G., Sandoval, C., Espinel, I., Sridhara, R., Aguilar, M., Guevara, A., Guderian, R.H., Levine, M.M., et al. (2000). Albendazole treatment of children with ascariasis enhances the vibriocidal antibody response to the live attenuated oral cholera vaccine CVD 103-HgR. J. Infect. Dis. *182*, 1199–1206.

Da'dara, A.A., and Harn, D.A. (2010). Elimination of helminth infection restores HIV-1C vaccine-specific T cell responses independent of helminth-induced IL-10. Vaccine *28*, 1310–1317.

Dawood, F.S., Iuliano, A.D., Reed, C., Meltzer, M.I., Shay, D.K., Cheng, P.Y., Bandaranayake, D., Breiman, R.F., Brooks, W.A., Buchy, P., et al. (2012). Estimated global mortality associated with the first 12 months of 2009 pandemic influenza A H1N1 virus circulation: a modelling study. Lancet Infect. Dis. *12*, 687–695.

Dietze, K.K., Dittmer, U., Koudaimi, D.K., Schimmer, S., Reitz, M., Breloer, M., and Hartmann, W. (2016). Filariae-Retrovirus Co-infection in Mice is Associated with Suppressed Virus-Specific IgG Immune Response and Higher Viral Loads. PLoS Negl. Trop. Dis. *10*, e0005170.

Dormitzer, P.R., Galli, G., Castellino, F., Golding, H., Khurana, S., Del Giudice, G., and Rappuoli, R. (2011). Influenza vaccine immunology. Immunol. Rev. *239*, 167–177.

Dzhivhuho, G.A., Rehrl, S.A., Ndlovu, H., Horsnell, W.G.C., Brombacher, F., Williamson, A.L., and Chege, G.K. (2018). Chronic schistosomiasis suppresses HIV-specific responses to DNA-MVA and MVA-gp140 Env vaccine regimens despite antihelminthic treatment and increases helminth-associated pathology in a mouse model. PLoS Pathog. *14*, e1007182.

Elias, D., Akuffo, H., and Britton, S. (2006). Helminthes could influence the outcome of vaccines against TB in the tropics. Parasite Immunol. *28*, 507–513.

Esen, M., Mordmüller, B., de Salazar, P.M., Adegnika, A.A., Agnandji, S.T., Schaumburg, F., Hounkpatin, A.B., Brückner, S., Theisen, M., Bélard, S., et al. (2012). Reduced antibody responses against Plasmodium falciparum vaccine candidate antigens in the presence of Trichuris trichiura. Vaccine *30*, 7621–7624.

Facciotti, F., Gagliani, N., Haringer, B., Alfen, J.S., Penatti, A., Maglie, S., Paroni, M., Iseppon, A., Moro, M., Crosti, M.C., et al. (2016). IL-10-producing forkhead box protein 3-negative regulatory T cells inhibit B-cell responses and are involved in systemic lupus erythematosus. J. Allergy Clin. Immunol. *137*, 318–321.

Feng, X., Classon, C., Terán, G., Yang, Y., Li, L., Chan, S., Ribacke, U., Rothfuchs, A.G., Coquet, J.M., and Nylén, S. (2018). Atrophy of skin-draining lymph nodes predisposes for impaired immune responses to secondary infection in mice with chronic intestinal nematode infection. PLoS Pathog. *14*, e1007008.

Floudas, A., Amu, S., and Fallon, P.G. (2016). New Insights into IL-10 Dependent and IL-10 Independent Mechanisms of Regulatory B Cell Immune Suppression. J. Clin. Immunol. *36* (*Suppl 1*), 25–33.

Furze, R.C., Hussell, T., and Selkirk, M.E. (2006). Amelioration of influenza-induced pathology in mice by coinfection with Trichinella spiralis. Infect. Immun. *74*, 1924–1932.

Gagliani, N., Magnani, C.F., Huber, S., Gianolini, M.E., Pala, M., Licona-Limon, P., Guo, B., Herbert, D.R., Bulfone, A., Trentini, F., et al. (2013). Coexpression of CD49b and LAG-3 identifies human and mouse T regulatory type 1 cells. Nat. Med. *19*, 739–746.

Garten, R.J., Davis, C.T., Russell, C.A., Shu, B., Lindstrom, S., Balish, A., Sessions, W.M., Xu, X., Skepner, E., Deyde, V., et al. (2009). Antigenic and genetic characteristics of swine-origin 2009 A(H1N1) influenza viruses circulating in humans. Science *325*, 197–201.

Graham, A.L., Taylor, M.D., Le Goff, L., Lamb, T.J., Magennis, M., and Allen, J.E. (2005). Quantitative appraisal of murine filariasis confirms host strain differences but reveals that BALB/c females are more susceptible than males to Litomosoides sigmodontis. Microbes Infect. *7*, 612–618.

Haben, I., Hartmann, W., Specht, S., Hoerauf, A., Roers, A., Müller, W., and Breloer, M. (2013). T-cell-derived, but not B-cell-derived, IL-10 suppresses antigen-specific T-cell responses in Litomosoides sigmodontis-infected mice. Eur. J. Immunol. *43*, 1799–1805.

Haben, I., Hartmann, W., and Breloer, M. (2014). Nematode-induced interference with vaccination efficacy targets follicular T helper cell induction and is preserved after termination of infection. PLoS Negl. Trop. Dis. *8*, e3170.

Hartmann, W., Haben, I., Fleischer, B., and Breloer, M. (2011). Pathogenic nematodes suppress humoral responses to third-party antigens in vivo by IL-10-mediated interference with Th cell function. J. Immunol. *187*, 4088–4099.

Hartmann, W., Schramm, C., and Breloer, M. (2015). Litomosoides sigmodontis induces TGF-β receptor responsive, IL-10-producing T cells that suppress bystander T-cell proliferation in mice. Eur. J. Immunol. *45*, 2568–2581.

Hoffmann, W., Petit, G., Schulz-Key, H., Taylor, D., Bain, O., and Le Goff, L. (2000). Litomosoides sigmodontis in mice: reappraisal of an old model for filarial research. Parasitol. Today (Regul.) *16*, 387–389.

Hotez, P.J., Brindley, P.J., Bethony, J.M., King, C.H., Pearce, E.J., and Jacobson, J. (2008). Helminth infections: the great neglected tropical diseases. J. Clin. Invest. *118*, 1311–1321.

Hussaarts, L., van der Vlugt, L.E., Yazdanbakhsh, M., and Smits, H.H. (2011). Regulatory B-cell induction by helminths: implications for allergic disease. J. Allergy Clin. Immunol. *128*, 733–739.

Kamanaka, M., Kim, S.T., Wan, Y.Y., Sutterwala, F.S., Lara-Tejero, M., Galán, J.E., Harhaj, E., and Flavell, R.A. (2006). Expression of interleukin-10 in intestinal lymphocytes detected by an interleukin-10 reporter knockin tiger mouse. Immunity *25*, 941–952.

Lahl, K., Loddenkemper, C., Drouin, C., Freyer, J., Arnason, J., Eberl, G., Hamann, A., Wagner, H., Huehn, J., and Sparwasser, T. (2007). Selective depletion of Foxp3+ regulatory T cells induces a scurfy-like disease. J. Exp. Med. *204*, 57–63.

Maines, T.R., Jayaraman, A., Belser, J.A., Wadford, D.A., Pappas, C., Zeng, H., Gustin, K.M., Pearce, M.B., Viswanathan, K., Shriver, Z.H., et al. (2009). Transmission and pathogenesis of swine-origin 2009 A(H1N1) influenza viruses in ferrets and mice. Science *325*, 484–487.

Maizels, R.M., and McSorley, H.J. (2016). Regulation of the host immune system by helminth parasites. J. Allergy Clin. Immunol. *138*, 666–675.

Mangan, N.E., Fallon, R.E., Smith, P., van Rooijen, N., McKenzie, A.N., and Fallon, P.G. (2004). Helminth infection protects mice from anaphylaxis via IL-10-producing B cells. J. Immunol. *173*, 6346–6356.

Maynard, C.L., Harrington, L.E., Janowski, K.M., Oliver, J.R., Zindl, C.L., Rudensky, A.Y., and Weaver, C.T. (2007). Regulatory T cells expressing interleukin 10 develop from Foxp3+ and Foxp3- precursor cells in the absence of interleukin 10. Nat. Immunol. *8*, 931–941.

McFarlane, A.J., McSorley, H.J., Davidson, D.J., Fitch, P.M., Errington, C., Mackenzie, K.J., Gollwitzer, E.S., Johnston, C.J.C., MacDonald, A.S., Edwards, M.R., et al. (2017). Enteric helminth-induced type I interferon signaling protects against pulmonary virus infection through interaction with the microbiota. J. Allergy Clin. Immunol. *140*, 1068–1078.

McSorley, H.J., and Maizels, R.M. (2012). Helminth infections and host immune regulation. Clin. Microbiol. Rev. *25*, 585–608.

Noland, G.S., Chowdhury, D.R., Urban, J.F., Jr., Zavala, F., and Kumar, N. (2010). Helminth infection impairs the immunogenicity of a Plasmodium falciparum DNA vaccine, but not irradiated sporozoites, in mice. Vaccine *28*, 2917–2923.

Osborne, L.C., Monticelli, L.A., Nice, T.J., Sutherland, T.E., Siracusa, M.C., Hepworth, M.R., Tomov, V.T., Kobuley, D., Tran, S.V., Bittinger, K., et al. (2014). Coinfection. Virus-helminth coinfection reveals a microbiota-independent mechanism of immunomodulation. Science *345*, 578–582.

Otte, A., and Gabriel, G. (2011). 2009 pandemic H1N1 influenza A virus strains display differential pathogenicity in C57BL/6J but not BALB/c mice. Virulence *2*, 563–566.

Otte, A., Sauter, M., Alleva, L., Baumgarte, S., Klingel, K., and Gabriel, G. (2011). Differential host determinants contribute to the pathogenesis of 2009 pandemic H1N1 and human H5N1 influenza A viruses in experimental mouse models. Am. J. Pathol. *179*, 230–239.

Reese, T.A., Wakeman, B.S., Choi, H.S., Hufford, M.M., Huang, S.C., Zhang, X., Buck, M.D., Jezewski, A., Kambal, A., Liu, C.Y., et al. (2014). Helminth infection reactivates latent γ-herpesvirus via cytokine competition at a viral promoter. Science *345*, 573–577.

Reese, T.A., Bi, K., Kambal, A., Filali-Mouhim, A., Beura, L.K., Bürger, M.C., Pulendran, B., Sekaly, R.P., Jameson, S.C., Masopust, D., et al. (2016). Sequential Infection with Common Pathogens Promotes Human-like Immune Gene Expression and Altered Vaccine Response. Cell Host Microbe *19*, 713–719.

Roncarolo, M.G., Gregori, S., Bacchetta, R., and Battaglia, M. (2014). Tr1 cells and the counter-regulation of immunity: natural mechanisms and therapeutic applications. Curr. Top. Microbiol. Immunol. *380*, 39–68.

Roncarolo, M.G., Gregori, S., Bacchetta, R., Battaglia, M., and Gagliani, N. (2018). The Biology of T Regulatory Type 1 Cells and Their Therapeutic Application in Immune-Mediated Diseases. Immunity *49*, 1004–1019.

Satoguina, J.S., Weyand, E., Larbi, J., and Hoerauf, A. (2005). T regulatory-1 cells induce IgG4 production by B cells: role of IL-10. J. Immunol. *174*, 4718–4726.

Satoguina, J.S., Adjobimey, T., Arndts, K., Hoch, J., Oldenburg, J., Layland, L.E., and Hoerauf, A. (2008). Tr1 and naturally occurring regulatory T cells induce IgG4 in B cells through GITR/GITR-L interaction, IL-10 and TGF-beta. Eur. J. Immunol. *38*, 3101–3113.

Schuijs, M.J., Hartmann, S., Selkirk, M.E., Roberts, L.B., Openshaw, P.J., and Schnoeller, C. (2016). The Helminth-Derived Immunomodulator AvCystatin Reduces Virus Enhanced Inflammation by Induction of Regulatory IL-10+ T Cells. PLoS ONE *11*, e0161885.

Smits, H.H., Hammad, H., van Nimwegen, M., Soullie, T., Willart, M.A., Lievers, E., Kadouch, J., Kool, M., Kos-van Oosterhoud, J., Deelder, A.M., et al. (2007).

Protective effect of Schistosoma mansoni infection on allergic airway inflammation depends on the intensity and chronicity of infection. J. Allergy Clin. Immunol. *120*, 932–940.

Su, Z., Segura, M., and Stevenson, M.M. (2006). Reduced protective efficacy of a blood-stage malaria vaccine by concurrent nematode infection. Infect. Immun. *74*, 2138–2144.

Urban, J.F., Jr., Steenhard, N.R., Solano-Aguilar, G.I., Dawson, H.D., Iweala, O.I., Nagler, C.R., Noland, G.S., Kumar, N., Anthony, R.M., Shea-Donohue, T., et al. (2007). Infection with parasitic nematodes confounds vaccination efficacy. Vet. Parasitol. *148*, 14–20.

van Riet, E., Adegnika, A.A., Retra, K., Vieira, R., Tielens, A.G., Lell, B., Issifou, S., Hartgers, F.C., Rimmelzwaan, G.F., Kremsner, P.G., and Yazdanbakhsh, M. (2007). Cellular and humoral responses to influenza in gabonese children living in rural and semi-urban areas. J. Infect. Dis. *196*, 1671–1678.

Wammes, L.J., Hamid, F., Wiria, A.E., May, L., Kaisar, M.M., Prasetyani-Gieseler, M.A., Djuardi, Y., Wibowo, H., Kruize, Y.C., Verweij, J.J., et al. (2016). Community deworming alleviates geohelminth-induced immune hyporesponsiveness. Proc. Natl. Acad. Sci. USA *113*, 12526–12531.

Wan, Y.Y., and Flavell, R.A. (2005). Identifying Foxp3-expressing suppressor T cells with a bicistronic reporter. Proc. Natl. Acad. Sci. USA *102*, 5126–5131.

World Health Organization (2019). Influenza.https://www.who.int/influenza/en/.

## STAR★METHODS

### KEY RESOURCES TABLE

| REAGENT or RESOURCE | SOURCE | IDENTIFIER |
|---|---|---|
| Antibodies | | |
| anti-mouse CD4-APC | Biolegend | clone RM4-5, Cat#100516; RRID:AB_312719 |
| anti-mouse CD4-BV510 | Biolegend | clone RM4-5, Cat#100553; RRID:AB_2563188 |
| anti-mouse CD19- BV711 | Biolegend | clone 6D5, Cat#115555; RRID:AB_2565970 |
| anti-mouse CD19- BV510 | Biolegend | clone 6D5, Cat#115546; RRID:AB_2562137 |
| anti-mouse LAG-3-APC | Biolegend | clone C9b7W, Cat#125210; RRID:AB_10639727 |
| anti-mouse CD49b-PE/Cy7 | Biolegend | clone HMa2, Cat#103518; RRID:AB_2566103 |
| anti-mouse Foxp3-AF700 | ThermoFisher Scientific | clone FJK-16S, Cat#56-5773-82; RRID:AB_1210557 |
| anti-mouse CTLA-4-PerCP Cy5.5 | Biolegend | clone UC10-4B9, Cat#106316; RRID:AB_2564474 |
| anti-mouse BTLA-PE | ThermoFisher Scientific | clone 6F7, Cat#12-5950-82; RRID:AB_466055 |
| anti-mouse PD-1-FITC | Biolegend | clone 29F.1A12, Cat#135214; RRID:AB_10680238 |
| anti-mouse TIGIT-PE/Dazzle™ 594 | Biolegend | clone 1G9, Cat#142110; RRID:AB_2566573 |
| anti-mouse TIM-3-BV421 | Biolegend | clone RMT3-23, Cat#134019, RRID:AB_2814028 |
| anti-mouse CD90.1-BV510 | Biolegend | clone OX7, Cat#202535; RRID:AB_2562643 |
| anti-mouse IL-10 APC | BD | clone JES5-16E3, Cat# 554468; RRID:AB_398558 |
| anti-mouse IL-10 receptor | Biolegend | clone 1B1.3A, Cat#112712; RRID:AB_2616680 |
| anti-mouse IgG1-HRP | ThermoFisher Scientific | Cat#04-6120; RRID:AB_2532940 |
| anti-mouse IgG2a-HRP | ThermoFisher Scientific | Cat#61-0220; RRID:AB_2533918 |
| anti-mouse IgG2c-HRP | Southern Biotech | Cat#1079-05; RRID:AB_2794466 |
| anti-mouse IgG2b-HRP | ThermoFisher Scientific | Cat#610320; RRID:AB_2533920 |
| anti-influenza A virus nucleoprotein | ThermoFisher Scientific | Cat#PA5-32242; RRID:AB_2549715 |
| anti-rabbit-Biotin | Jackson ImmunoResearch | Cat#711-066-152; RRID:AB_2340594 |
| Bacterial and Virus Strains | | |
| Influenza A A/Hamburg/NY1580/09 | provided by Prof. G. Gabriel (HPI, Hamburg, Germany) | Otte et al., 2011 |
| Chemicals, Peptides, and Recombinant Proteins | | |
| $OVA_{323-339}$ | JPT peptide Technologie | Sequence: ISQAVHAAHAEINEAGR |
| Diphtheria Toxin | Calbiochem | Cat#322326 |
| PMA | Sigma-Aldrich | Cat#79346-1MG |
| Ionomycin | Sigma-Aldrich | Cat#I9657-1MG |
| Brefeldin A Solution (1000x) | Biolegend | Cat#420601 |
| Monensin Solution (1000x) | Biolegend | Cat#420701 |
| Tetramethylbenzidine | Carl Roth | Cat#635.02 |
| Trypsin-EDTA | Biozym | Cat#BE17-161E |
| TPCK Trypsin | Sigma | Cat#T1426-50mg |
| Tween 20 | Carl Roth | Cat#9127.2 |
| Crystal violet | Merck | Cat#101408 |
| Avicel | FMC | Cat#9004-32-4 |
| Formaldehyde 37% | Carl Roth | Cat#4979.1 |
| Dimethyl sulfoxide | Sigma-Aldrich | Cat#D5879-500ML |
| Bovine Serum Albumin (BSA) | Sigma-Aldrich | Cat#A7979-50ml |
| BSA | Serva | Cat#11930.03 |

(*Continued on next page*)

*Continued*

| REAGENT or RESOURCE | SOURCE | IDENTIFIER |
|---|---|---|
| Minimum Essential medium | Lonza | Cat#12-668E |
| Penicilin/Streptomycin | Biozym | Cat#882082 |
| carboxyfluorescein succinimidyl ester | ThermoFisher Scientific | *Cat#65-0850-84* |
| Critical commercial Assays | | |
| Foxp3 / Transcription Factor Staining Buffer Set | ThermoFisher Scientific | Cat#00-5523-00 |
| LEGENDplex Mouse Th cytokine panel | Biolegend | Cat#740005 |
| Avidin / Biotin Blocking Kit | Biozol | Cat#VEC-SP-2001 |
| ZytoChemPlus-HRP- Kit, Broad Spectrum | Zytomed | Cat# HRP008DAB |
| MojoSort Mouse CD4 T Cell Isolation Kit | Biolegend | Cat#480033 |
| Zombie UV Fixable Viability Kit | Biolegend | Cat#423108 |
| Zombie Aqua Fixable Viability Kit | Biolegend | Cat#423102 |
| MagniSort Mouse CD4 T cell Enrichment Kit | ThermoFisherScientific | Cat#8804-6821-74 |
| Experimental Models: Cell lines | | |
| MDCK cells | provided by Prof. G. Gabriel (HPI, Hamburg, Germany) | N/A |
| Experimental Models: Organisms/Strains | | |
| C57BL/6 mice | BNITM or Janvier Labs | N/A |
| BALB/c mice | BNITM or Janvier Labs | N/A |
| Fir/TIGER mice | provided by Prof. N. Gagliani (UKE, Hamburg, Germany) | N/A |
| 10BiT mice | provided by Profs. C. Weaver (University of Alabama, USA) and N. Gagliani (UKE, Hamburg, Germany) | N/A |
| DEREG mice | BNITM | N/A |
| OT-II mice | BNITM | N/A |
| *Litomosoides sigmodontis* | BNITM | N/A |
| Cotton rats | BNITM | N/A |
| Software and Algorithms | | |
| FACS Diva | Becton Dickinson | N/A |
| FlowJo | TreeStar, Mountain View, CA | https://www.flowjo.com |
| Graph Pad Prism | GraphPad Software | https://www.graphpad.com/ |
| Adobe Photoshop CS5.1 | Adobe Systems Incorporated | https://www.adobe.com/ |
| Other | | |
| Chicken blood | Lohmann Tierzucht GmbH | https://www.ltz.de/de/ |
| Begripal (season 2014/15 and 2016/17) | Seqirus | N/A |

## LEAD CONTACT AND MATERIALS AVAILIBILITY

Further information and requests for resources and reagents should be directed to and will be fulfilled by the Lead Contact, Minka Breloer (breloer@bnitm.de). This study did not generate new unique reagents.

## EXPERIMENTAL MODEL AND SUBJECT DETAILS

### Mice

All mouse experiments were conducted at the specific pathogen-free animal facility of the Bernhard Nocht Institute for Tropical Medicine (BNITM) in agreement with the German Animal Welfare Act and the relevant German authority (Behörde für Gesundheit und Verbraucherschutz, Hamburg, approval numbers 84/15, 103/2018). All mice were kept in individually ventilated cages (maximum of 5 mice per cage). For experiments gender-matched adult (8-12 weeks) male and female mice were used. C57BL/6 and BALB/c mice were either bred in the animal facility of the BNITM or were obtained from Janvier Labs. OT-II and C57BL/6 DEREG mice

were bred at the BNITM. DEREG mice express green fluorescent protein (GFP) and the human diphtheriatoxin (DT) receptor as fusion protein under the control of the Foxp3 gene locus (Lahl et al., 2007). Non-transgenic littermates from the DEREG breeding were used as C57BL/6 control mice. C57BL/6 DEREG and C57BL/6 control littermates received 1 μg Diphteriatoxin (DT) i.p. either one day before and two days after *L. sigmodontis* infection or one day before and one day after vaccination. In two out of three experiments Fir (Foxp3-IRES-mRFP)/TIGER (interleukin-ten-ires gfp-enhanced reporter) mice were used. In Fir mice monomeric red fluorescent protein (mRFP) is knocked in the endogenous Foxp3 locus (Wan and Flavell, 2005). TIGER mice are knock-in mice where an internal ribosome entry site (IRES) green fluorescent protein (GFP) was inserted in front of the IL-10 gene (Kamanaka et al., 2006). In another experiment (day 30 p.i.) IL-10-Foxp3 double reporter mice with an additional IL-4 reporter were used. The 10BiT (IL-10 BAC-in transgene) mice express the transgene Thy1-1 (CD90.1) under the control of IL-10 (Maynard et al., 2007) which allows detection of IL-10 competent cells by staining for CD90.1. Foxp3 was detected as mRFP.

### Cell Culture

Madin Darby canine kidney (MDCK) cells were cultured in RPMI medium supplemented with 10% FCS, 2 mM Glutamin and 1% Penicilin/Streptomycin. For the Plaque Assay Minimum Essential medium without Phenol Red supplemented with 0.5% BSA, 2 mM Glutamin, 20 mM HEPES and 1% Penicilin/Streptomycin. Cells were grown at 37°C in a 5% $CO_2$ incubator.

## METHOD DETAILS

### L. sigmodontis and influenza infection

The life cycle of *L. sigmodontis* was maintained in their natural reservoir, the cotton rats (*Sigmodon hispidus*). Therefore cotton rats were anesthetized and blood was collected from the retro-bulbar sinus in order to count L1. Cotton rats, which were used for further infection of blood-sucking mites (*Ornithonyssus bacoti*), had an infection rate of 500 – 2000 L1 per μl blood. Infected cotton rates were exposed to mites that ingested L1 during a blood meal. Infected mites were kept at 29°C and 90% humidity for 14 days to allow maturation of L1 to L3. Experimental mice were anesthetized and exposed to these infected mites for 16 hours, i.e., naturally infected. To verify the worm burden in infected mice, the TC was flushed with 10 mL PBS.

For influenza infection mice were anesthetized with ketamine/xylazine (100 and 5 mg/kg) and i.n. infected with 25 μL $1 \times 10^3$ (C57BL/6) or $1 \times 10^4$ (BALB/c) plaque forming units (PFU) 2009 pH1N1 influenza A/Hamburg/05/09 virus. The influenza virus was isolated from pharyngeal swabs of a female patient as described previously (Otte et al., 2011). Health status of the mice was monitored daily according to the animal protocols approved by the Hamburg authorities. Body weight was measured at the indicated time points of infection either until non-vaccinated mice regained their original body weight or until day 3 p.i. if mice were sacrificed to analyze viral burden and IL-6 content in the lung.

### Vaccination and quantification of the vaccine-specific humoral response

Mice were vaccinated by i.p. injection of 3.75 μg non-adjuvanted vaccine against influenza season 2014/15 and 2016/17 (Begripal, Seqirus) in 200 μL PBS. In indicated experiments IL-10R signaling was blocked by i.p. application of 200 μg anti-mouse IL-10 receptor mAb (Biolegend) one day before vaccination and on days 1, 3, 6, and 9 post vaccination. At indicated time points 2-4 weeks after vaccination blood was collected from the vena fascialis and allowed to coagulate for 1h at RT. After centrifugation (10.000 x g for 10 min) serum was transferred into a fresh tube and stored at −20°C until further analysis.

### Quantification of HA-specific IgG

ELISA High Binding Microlon (Greiner, Cat#655061) plates were coated overnight with 1 μg/mL Begripal. Plates were washed and blocked for 2 h with 100 μL 1% BSA (Serva) in PBS. After 2 h incubation with serially diluted serum in duplicates, plates were washed and incubated for 1 h with HRP-labeled anti-mouse IgG1, IgG2a, IgG2c, and IgG2b. After a further washing step, plates were developed with 100 μL tetramethylbenzidine (0.6 mg/mL in DMSO), 0.003% $H_2O_2$ in 100mM $NaH_2PO_4$ (pH 5.5) for 2.5 min. Reaction was stopped by addition of 25 μL 2 M $H_2SO_4$ per well and $OD_{450}$ was measured. The titer is defined as the last serum dilution that results in an $OD_{450}$ above the double background.

### Hemagglutinin inhibition (HI) assay

Murine serum samples were thawed and heat inactivated for 30 min at 56°C in a water bath. Serial dilutions of sera in 25 μL PBS were incubated with 25 μl of 2009 pH1N1 influenza A virus in duplicates in 96-well-V-plates (Greiner, Cat#651101). The virus solution was standardized to 8 hemagglutination units before. After 30 min incubation at room temperature, 50 μL 1% fresh chicken red blood cell solution in 0.9% NaCl was added to each well. The dilution that still inhibited agglutination was calculated as a titer after a further 1-hour-incubation at 4°C.

### Detection of viral loads and IL-6 in the lungs

Viral loads were determined in lung homogenates by MDCK plaque assay. At day 3 post influenza infection, lungs were removed and homogenized in 0.1% BSA in PBS. The supernatatant was collected after centrifugation (10 min, 950 x g, 10 min, 4°C) and stored at −80°C. Serial dilutions of lung homogenates ($10^1$ to $10^{5)}$ were added to a confluent MDCK cell culture in 6-well-plates (Greiner,

Cat#657 960). After 30 min at 37°C, plates were overlaid with 3 mL 1.25% Avicel in MEM containing 1μg/mL tolylsulfonyl phenylalanyl chloromethyl ketone (TPCK)-Trypsin. After a further incubation for 72 h at 37°C and 5% $CO_2$, the overlay was removed and the plates were washed with PBS. The cells were fixed with 0.5 mL 4% paraformaldehyde (PFA) for 30 min at 4°C. PFA was removed and plates were incubated for 10 min with 1 mL/well 1% crystal violet. The staining was stopped by removing crystal violet and washing the plates with tap water. IL-6 in lung homogenates was quantified by LEGENDplex Mouse Th cytokine panel (13-plex, Biolegend) after virus inactivation for 30 min at 56°C according to the manufacturers recommendation.

### Histology

At day 3 post influenza infection, lungs were removed, fixed in 4% PFA and stained immunohistochemically against influenza virus antigen using antibody against rabbit anti-influenza A virus nucleoprotein (Thermo Fisher Scientific) which were detected by a biotin-conjugated anti-rabbit secondary antibody, the Avidin/Biotin Blocking Kit, and the ZytoChemPlus-HRP-Broad Spectrum (diaminobenzidine) Kit, according to the manufacturer's instructions. Images were acquired using a Nikon Eclipse Ti with an objective 2x 0.10 (NIKON, Tokyo, Japan). Image processing was performed using Adobe Photoshop CS5.1. Histopathological analysis was performed in a blinded manner.

### Flow cytometry

For intracellular IL-10 staining spleen cells were stimulated for 4 h with 500 ng/mL Phorbol 12 myristate 13-acetate (PMA) and 500 ng/mL Ionomycin in the presence of Brefeldin A (1x) and Monensin (1x). Single cells ($3 \times 10^6$) from the spleen or TC were stained with 1 μL Zombie UV Fixable Viability Kit or Zombie Aqua Fixable Viability Kit in 1 mL PBS for 30 min at 4°C. For surface staining, cells were first stained for 15 min at 37°C with anti-mouse APC-labeled anti-mouse LAG-3 and PE/Cy7-labeled anti-mouse CD49b. After an additional incubation for 15 min at RT, cells were washed and stained for 30 min on ice with FITC-labeled antibodies against mouse PD-1, PE-labeled anti-mouse BTLA, PE/Dazzle 594-labeled anti-mouse TIGIT, BV421-labeled anti-mouse TIM-3, APC- or BV510-labeled anti-mouse CD4, BV711-labeled or BV510 anti-mouse CD19. IL-10 expression in IL-10/Foxp3/IL-4 reporter mice was quantified by counterstaining the expression of IL-10 with an anti-CD90.1 BV510 Ab. For subsequent intracellular staining with anti-mouse AF700-labeled anti-mouse Foxp3, PerCP Cy5.5-labeled anti-mouse CTLA-4, and APC-labeled anti-mouse IL-10 Ab, cells were fixed and permeabilized with Thermofisher Scientific Foxp3/Transcription factor staining buffer set according to the manufacturer's protocol. Samples were analyzed on a LSRII or a LSRFortessa (Becton Dickinson) using FlowJo software (TreeStar). For the cluster analysis data were analyzed using tSNE, a dimensionality reducing plugin for Flow Jo. Data were gated on $CD4^+$ single cells and downsampled to 30,000 events per sample. Heatmaps from the tSNE analysis show the expression intensity of Foxp3, PD-1, LAG-3, CD49b, BTLA, CTLA-4, TIGIT, and TIM-3.

### Analysis of OT-II cell proliferation *in vivo*

OVA-specific T cells were isolated from the spleens of OT-II mice using MojoSort Mouse CD4 T Cell Isolation Kit (Biolegend) or MagniSort Mouse CD4 T cell Enrichment Kit (ThermoFisher Scientific) according to the manufacturers instructions. Isolated OT-II T cells were stained with carboxyfluorescein succinimidyl ester (CFSE, ThermoFisher Scientific). $5 \times 10^7$ cells were diluted in 10 mL sterile PBS and incubated at 37°C with 5 μM CFSE. The amount of CFSE was, if required, adjusted to the number of cells. After 10 min the reaction was stopped by addition of 40 mL of 3% FCS in PBS. Cells were washed twice. CSFE-labeled transgenic OT-II T cells ($2 \times 10^6$) were injected in 200 μl PBS intravenously into non-infected mice or mice that had been infected with *L. sigmodontis* infection 14 or 90 days earlier. One day after the transfer OT-II T cells were activated by the injection of 30 μg $OVA_{323-339}$ (JPT peptides) i.p. Mice were sacrificed 72 h after the cell transfer. Spleen cells were isolated and stained with APC-labeled anti-CD4 Ab (Biolegend, clone: RM4-5). Proliferating cells were defined as $CFSE^{low}$ as shown in Figure S3).

## QUANTIFICATION AND STATISTICAL ANALYSIS

### Statistical analysis

Data were analyzed using Graph Pad Prism, testing for normality distribution and further tested either with Student t test (parametric) or Mann-Whitney-U test (non parametric) comparing two groups to each other. For comparison of more than two groups to each other either 1-way ANOVA with Bonferronís multiple comparison test (parametric) or Kruskall-Wallis with Dunns multiple comparison test (non parametric) were performed. For comparison of body weight changes over time between 2 groups the 2-way ANOVA was performed. Statistical tests are indicated in the Figure legends. Asterisks for all analyses *$p \leq 0.05$, **$p \leq 0.01$, ***$p \leq 0.001$, ****$p \leq 0.0001$.

## DATA AND CODE AVAILABILITY

The published article includes all datasets generated or analyzed during this study.